COMPARITIVE NONLINEAR FINITE ELEMENT ANALYSIS OF SQUARE AND CIRCULAR STEEL BASE PLATE ON LEVELING NUTS USING ANSYS

A Thesis

Submitted in partial fulfillment of the requirements for the award of the degree of

MASTER OF TECHNOLOGY

IN

CIVIL ENGINEERING

With specialization in

STRUCTURAL ENGINEERING

Under the supervision of

Dr. Ashok Kumar Gupta

(Head of Department)

&

Mr. Kaushal Kumar

(Assistant Professor)

By

Sumer R Singh

(162656)

To

JAYPEE UNIVERSITY OF INFORMATION TECHNOLOGY
WAKNAGHAT, SOLAN – 173 234
HIMACHAL PRADESH, INDIA

MAY-2018

CERTIFICATE

This is to certify that the work which is being presented in the thesis entitled **"COMPARITIVE NONLINEAR FINITE ELEMENT ANALYSIS OF SQUARE AND CIRCULAR STEEL BASE PLATE ON LEVELING NUTS USING ANSYS"** in partial fulfillment of the requirements for the award of the degree of Master of Technology in Civil Engineering with specialization in "**Structural Engineering**" and submitted to the Department of Civil Engineering, Jaypee University of Information Technology, Waknaghat is an authentic record of work carried out by **Sumer R Singh** (Enrolment No. 162656) during a period from July 2017 to May 2018 under the supervision of **Dr. Ashok Kumar Gupta** (Head of Department) and **Mr. Kaushal Kumar (**Assistant Professor), Department of Civil Engineering, Jaypee University of Information Technology, Waknaghat.

The above statement made is correct to the best of our knowledge.

Date:

Dr. Ashok Kumar Gupta	Mr. Kaushal Kumar	External Examiner
Professor & Head of Department	Assistant Professor	
Department of Civil Engineering	Department of Civil Engineering	
JUIT Waknaghat	JUIT Waknaghat	

ACKNOWLEDGEMENT

I extend my heartily gratitude to my Project Guide Dr. Ashok Kumar Gupta (H.O.D. Civil) and Mr. Kaushal Kumar (Assistant Professor) for his constant guidance and support in pursuit of this project. They have been a true motivation throughout and helped me in exploring various horizons of this project. Without their guidance, this project wouldn't have been possible. I would also like to thank my colleagues for their co-operation in framing the project.

Date: Sumer R Singh

M.Tech- Structural Engineering 2^{nd} year (4^{th} semester)

ABSTRACT

Base plates are used to connect structural members to their foundations. They are routinely used in cantilevered structures supporting traffic utilities like overhead cantilevered direction signboards, traffic signals, speed cameras and high mast roadway light poles as well as in industrial warehouses and garages. These poles are usually supported on concrete footings by means of steel base plates on levelling nuts. The purpose of the leveling nuts is to adjust alignment of the supported member. Currently, there are no simple design methods in the relevant structural codes. Therefore, the objective of the proposed study is to compare the square and base plate of same thickness under same type and magnitude of loadings. To accomplish the stated objective, the base plates of different thicknesses and subjected to three types of loading: Concentric loading, Uniaxial loading and Biaxial loading were analysed using ANSYS software. The results of total deformation, equivalent stress, maximum principal stress, minimum principal stress and maximum shear stress were obtained from ANSYS software. These results were finally obtained and comparative study between square base plate and circular base plate was conducted. It was observed that circular plate showed better results for above parameters under similar loading, thickness and plate area.

Keywords: ANSYS, Base plate.

TABLE OF CONTENTS

LISTS OF FIGURES

LIST OF TABLES

CHAPTER 1

INTRODUCTION

1.1 Nonlinear Analysis:

Analysis methods where linear-elasticity is accepted are known as first-order elastic analyses. This implies a linear association between forces and displacements and that the stress-strain relationship of the material is linear. With the exordium of design codes that require second-order analyses, the emphasis on analysis methods will definitely shift to second order elastic-plastic analyses. The assimilation of semi-rigid connections is also advisable, as this is a further step in the modeling of the real behavior of structural plane steel frames [18].

Nonlinear analysis can be of several types:

1.1.1 Material Nonlinearity:

The source of material nonlinearities is kindred to the components of a system, namely concrete and steel [18].

Concrete:

Concrete is a brittle material with dissimilarly different responses in tension and compression. In tensile stiffness and strength are small, and design codes typically ignore them. Under compressive stresses, the concrete stiffness de-escalates significantly 0.5 times concrete strength in uniaxial compression [18].

Steel*:*

Steel shows elastoplastic behavior in both tension and compression. Moreover, steel members hold residual stresses due to fabrication or erection processes. Connection between steel and concrete constituent contributes to the nonlinearity of a composite system because the different components may exhibit complicated and highly nonlinear behavior [18].

1.1.2 Geometric Nonlinearity:

Geometric nonlinearities are generally categorized into global and load nonlinearities. Global geometric nonlinearities often referred to as P-Delta effect, maybe incorporated in global models following basic procedures used in nonlinear frame analysis (McGuire et al 1999). Although usually neglected in frame analysis, local buckling of steel component, we considered in more improved finite element analysis that warrants the inclusion of such behavior [18].

*1.1.3 **Connection Nonlinearities**:*

A connection is a medium over which forces and moments are transferred from one member to another, such as from a beam to a column. For a beam-to-column connection in a plane frame, the primary forces transferred from the beam to the column embrace axial force, shear force and bending moment. For most connections the axial and shear deformations are relatively small equated with rotational deformation. The rotational deformation is set as a function of the moment in the connection. When a moment, M, is applied to a connection, a relative rotation (Theta), happen between the beam and the column. This rotation describes the change in angle between the beam and the column. When staged on a graph of moment (M) against relative rotation (Theta) (*Fig. 1.1*) the actions of a simple connection are represented by the Theta-axis. The actions of the fully-rigid connection are represented by the M-axis with Theta axis. All semi-rigid connections are represented by curves lying between these two extremes, allowing some moment to be transferred and some rotation to betide in a connection [18].

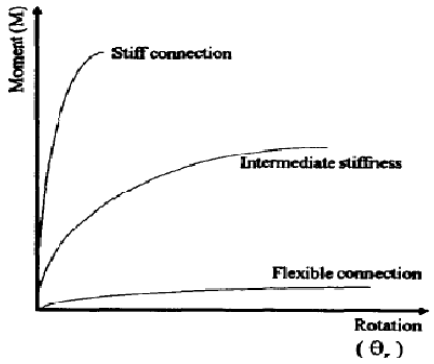

Fig-1.1: Moment-rotation curve [18].

1.2 Base Plate:

Base plates with leveling nuts are constantly used for structural supports for highway signs, luminaries, traffic signals, and stadium light poles. They are also accustomed in industrial warehouses, garages, airports and railway facilities. Such poles with base plates are also accustomed as light poles in recreation parks, sport fields, and outdoor stadiums. These utility poles are popularly supported on concrete footings by means of steel base plates on leveling nuts, as shown in *Fig. 1.2* [18].

The aim of the leveling nuts is to provide means for adjusting the alignment and final elevation at the top of the structure. The applied loading on utility structures bring about membrane, flexural, and shear stresses in the steel plate, due to gravity (self-weight) and lateral loads (wind/earthquake loads). Before a base plate can be designed, a section modulus, which is a function of a portion of the plate width times the square of the plate thickness, must be set in order to calculate the bending stresses in the base plate. Presently, there is no rational approach for determining the effective width of the plate to be used in the section modulus formula. Most engineers count on either approximate or conservative methods that are often not rationally-based, or they use expensive/time consuming refined methods of analysis [18].

Generally, after leveling of base plates the clear spacing beneath the plate is grouted or left empty, see *Fig. 1.3*: Hong Kong airport rail link. Experience has exhibited that the grout under the base plate cannot be counted on due to its low strength and durability, making it susceptible to cracks with time due to the severe environmental effects. When ungrouted, the spacing beneath the base plate is kept clear of debris and sand in case when future adjustments using leveling are expected on regular basis. The leveling nuts also contribute the added flexibility of replacing the damaged pole in case the foundation is not affected after a storm or accident [1]. The stiffness of semi-rigid connections is given by the slope of the moment-rotation curve as shown in *Fig.-1.1* [18].

Base plates are used to distribute the load from a steel column over the concrete foundation. The column base plates may be subjected to three types of loading, depending on the eccentricity of the load. They are: (1) Axial load only; (2) axial load plus a relatively small moment; and (3) axial load plus a relatively large moment. In the first case and sometimes in the second case, the entire area of the base plate is under compressive pressure [14].

Fig. 1.2: Utility pole at a park [1].

Fig. 1.3: Hong Kong airport rail link [1].

In practice, a thicker base plate is more frugal than a thinner base plate with additional stiffeners or other reinforcements (DeWolf1990). Base plates shall favorably be fabricated from Fe 250 steel due to their high ductility demand. Anchor rods are often cast in place, but may here and there be drilled into the hardened concrete. Minimum embedment length of anchor rods is most commonly taken 12 times their diameter (Fisher and Klaiber 2003). When more strength is required from the anchors, the diameter is usually increased before switching to higher grades. Non-shrink grout is sometimes used under base plates to fill up the empty space beneath the base plate and prevent corrosion and deterioration of the base plates and anchor bolts [1].

1.3 Problem Statement:

Utility poles in industrial facilities and steel columns in building structures are most commonly supported on concrete footings by means of steel base plates. The base plates are welded to the bottom of the steel poles or columns. The plates are attached to the footings with the help of anchor bolts and the space between the base plate and the concrete foundation is often left ungrouted. But even if there is grout under the base plate, it cannot be taken that the grout can support the plate as it is prone to crack with temperature changes and shrinkage effects. There is limited research on the behavior of base plates seated on leveling nuts, although this is the preeminent method used for supporting steel structures in the utility industry [1].

Early failure of such assemblies has often caused fatalities and is hazard to public safety. In the last five years, at least 80 defective existing poles have been taken down in Texas only because of cracks and other signs of structural failure. About 33% of signal supports audited in United States were having cracks in either the base plates or the concrete foundation (FHWA 2005). There has been very limited research on column bases as analogized to beam to column connections. Moreover, most of the published work on base plates addresses steel plates in contact with the concrete exterior of the foundation. Based on the above, there is a strong want for investigating this issue with experimental testing and computational studies. The schematic diagram for utility pole is shown in *Fig: 1.4* [1].

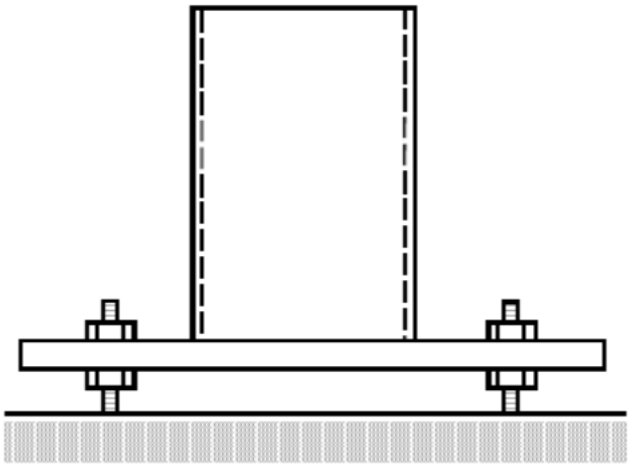

Fig. 1.4: Base Plate column connection schematic detail [1].

1.4 Research Objectives:

1. To study and analyze the behavior of square and circular base plate with change in number of anchor rods, change in type of loading (concentric, uniaxial and biaxial) and change in plate thicknesses by calculation of total deformation, equivalent stress, maximum principal stress, minimum principal stress and maximum shear stress.
2. Use the results obtained from the study and analyses to compare square and circular base plates and find the better of these two plates for various results like total deformation, equivalent stress, maximum principal stress, minimum principal stress and maximum shear stress.

1.5 Scope of Study:

The important parameters considered in this study are:

1. Nature of applied load (concentric versus eccentric loading).

2. Number of bolts.

3. Spacing between bolts.

4. Distance between the bolts and face of the column.

5. Size of the tubular column.

6. Dimensions of the base plates including the thickness.

1.6 Significance of Study

Steel utility poles supported on leveling nuts are becoming more prevalent worldwide thanks to improvements in corrosion prevention and lower production costs. Such a system is critical since it does not have a high level of redundancy. Enhancing the engineering design aspect of these structures will result in optimized designs based on a rational approach and reduce premature failures due to lack of understanding of their structural behavior [1].

CHAPTER 2

LITERATURE REVIEW

2.1 Introduction:

This chapter presents a summary of different studies on the behavior and design of steel base plates on leveling nuts. It includes procedures and guidelines of steel base plates by different authors along with recently completed experimental and computational studies available in the published literature.

2.2 Previous Studies:

Patel K and Chen W [21]:

In the paper "Nonlinear Analysis of Steel Moment Connection" a nonlinear stress analysis was performed on a flange connection plate by isolating it with suitable free body. The weld required to join the flange connection plates to the column was proposed through the study of stress distribution in the flange connection plate. For finite element modelling a general purpose Non-linear structural analysis program (NONSAP) was used for the analysis.

Thambiratnam D and Paramasivam P [20]:

In the paper "Base plates under axial loads and moments" experiments were conducted by applying axial loads and moments by eccentric loading on the column to study the behaviour of base plates. Thickness and eccentricity of the loads were the parameters of the study. At higher eccentricities the mode of failure observed was due to yielding of base plate and at lower eccentricities the primary mode of failure was due to cracking of plate. From the experiments it was observed that the eccentricity of base plate has greater influence on the strain than the thickness of the base plate. The test results showed that the base plate

at higher eccentricities failed due to yielding and that the behaviour of the base plate under testing is somewhat different form the design methods.

Wong M and Loi F [19]:

In the paper **"**Analysis of frames involving geometrical and material nonlinearity**"** a simpler procedure about framed structure is presented for solving the fully nonlinear problem. The basis of this procedure is a direct combination of two separately developed formulation and these are for large deformation purely elastic analysis and for small displacement elastic-perfectly plastic analysis. Path linearization scheme was proposed to link the two parts. The main emphasis of this paper was to explain how the two procedures are combined.

A general computer program NONPLAST was also briefly described. A three-stage process of a general finite element approach was proposed to perform the combined geometrical and material nonlinear analysis. Following it is the second stage of path linearization which links two types of analysis. Finally, an appropriate method for the incremental path dependent computer analysis of elastic-perfectly plastic frames inclusive of large deformations was used. Also, geometrical nonlinear analysis was combined through a path linearization technique to a small displacement elasto-plastic analysis.

Kruger et al [18]:

In the paper "Nonlinear analysis of structural steel frames" various ways of including material, geometrical and connection nonlinearities into a stiffness matrix was discussed. The stiffness matrix method was adjusted to incorporate all these nonlinearities into software which was developed by the author. Finally, by the means of computer program an example was illustrated.

Najjar S and Burgess I [17]:

In the paper "A nonlinear analysis for three-dimensional steel frames in fire conditions" a program '3DFIRE' based on principles of frame analysis was developed for modelling the behavior of skeletal frames under fire conditions. This particular program is based on another program 'INSTAF' which is used for nonlinear spread of yield analysis of

rigid frameworks. The same was modified to a 3-D capability covering both geometric and material nonlinearities, including effect of temperature variations on material properties.

Ermopolous J and Stamatopoulos G [16]:

In the paper "Mathematical modelling of column base plate connections" a design procedure was proposed for the derivation of Moment-rotation curves of column base connections which was based on classical design. Also, a new formula was proposed which describes the relation between moment and rotation with adequate accuracy.

Stamatopoulos G and Ermopoulos J [15]:

In the paper "Interaction curves for column base-plate connections" by taking into account the main parameters of the problems the ultimate behaviour of column base-plate connections is studied and the corresponding M-P curves were obtained. The parameters considered were the size and thickness of the plate, the size, length and location of anchor rods, the amount of axial load on the column and the quality of material used. Finally form the M-P curves the safety of the connections was checked.

Thevendran et al [14]:

In the paper "Nonlinear analysis of steel-concrete composite beams curved in plan" behavior of steel-concrete composite beams curved in plan are dealt with. The study of nonlinear behavior and ultimate load carrying capacity of such beams was done using finite element program 'ABAQUS'. The behavior of concrete slab and steel girder were simulated using shell elements and shear stud elements were simulated using rigid beams. Finally, a comparison was drawn between the proposed finite element model and the available experimental results to validate the results.

Drake R and Elkin S [13]:

In the paper "Beam-Column base plate design – LRFD method" a methodology for the design of beam-column base plates and anchor rods using factored load directly in the manner consistent with the equation of equilibrium and LFRD specification were represented. Two design examples were presented and a comparison was made with the problem solved by another AISC method. Finally, it was concluded that uniform rectangular

pressure distribution will be easier to design and program than the linear triangular pressure distribution utilized in allowable stress design and other published LFRD publications.

Sebastian W and McConnel R [12]:

In the paper "Nonlinear finite element analysis of steel-concrete composite structure" the elements used to represent the concrete slab and steel beam actions are described. Also, a demonstration on how to model ribbed composite slabs of reinforced concrete on profiled steel sheeting was done. Attention was drawn to the usefulness of layering technique to decide local stress redistribution associated with progressive through-depth cracking and yielding in the slab and steel beam elements. Predicted crack patterns and the use of the program gave the desired results and these are used to compare very well with those from experiments on reinforced concrete slabs and steel-concrete composite structures up to failure.

Liew et al [10]:

In the paper "Inelastic analysis of steel frames with composite beams" method was described for inelastic analysis of frames with composite floor beams subjected to the combined action of gravity and lateral loads. To model the composite beams based on moment-curvature relationship am inelastic formulation was proposed and to model steel columns plastic hinge approach was proposed. For the accuracy of these models two composite beams and steel portal frames were analyzed and results for the same were compared with the test results. Finally, the study showed that the limit load of steel frames while considering the composite beam effect is about 30% higher than pure steel frame.

Chan [9]:

In the paper "Non-Linear behavior and design of steel structures" the summary and reviews of various works conducted on the non-linear analysis and design of steel frames in past few decades was addressed. Finally, with the design procedure NIDA (developed by Chan) it was recognized that the elastic approach is not an economical design due to the ignorance of reserved strength after first yield or first plastic hinge.

Hag-Elsafi et al [8]:

In the paper "New procedure for design of end plates and base plates of cantilevered traffic support structures" a new procedure was developed for design of end plates and base plates, and for base plates of span-wire-mounted traffic-signal structures. The procedure developed was based on beam-and-plate bending and torsion theory. Also, the procedure developed was intended for plates of square configuration. Finally, the plate stresses and thickness obtained from the procedure were compared well with those estimated from finite element analysis and supported earlier conclusions reached through physical testing.

Spacone E and Tawil S [7]:

In the paper "Nonlinear analysis of steel-concrete composite structure" the focus was on the frame elements. First section models were presented (resultant and fiber models). Models with lumped and distributed inelasticity were covered. Partially restrained and rigid joints were reviewed and discussed at length. Modelling application of the analysis of composite frames was also presented. This paper was the State of the art review on composite structures.

CHAPTER 3

METHODOLOGY

3.1 Introduction to Finite Element Method:

The finite element method is a numerical process for solving problems of engineering and physics. In cases concerning complex geometries, loadings, material properties and boundary conditions, it is not easy to find analytical solutions. The analytical solutions in such cases demands solving ordinary or partial differential equations with many unknowns. Hence numerical methods, such as the finite element or finite difference method, are needed to figure out such problems. In the finite element method, the object is divided into numerous smaller bodies or elements and interconnected at common points called nodes or boundary lines. Each of the fine elements is solved separately using algebraic equations and the unknowns are calculated. The solution of all the elements is unified to obtain the solution of the object under study. In structural cases, the unknowns are displacements or stresses created by the applied force. These stresses and displacements are found at each node comprising the element, with each element making up the structure that is subjected to load [1].

Finite element analysis is a piecemeal solution. The basic approach of a piecemeal solution is to consider a body subjected to force and displacement boundary conditions that are changing. We delineate the externally applied forces and displacement boundary condition as functions of time. Since we are expecting non-linearity in the body therefore we account for load steps. However, it must be kept in mind that the time is only pseudo-variable, only signifying the load level and the material properties are time-independent (Bathe 1982). The load should be same at end of each step regardless of time itself. Time-dependent material properties are such as creep trouble. In this case load steps must be very cautiously chosen. At the end of each time step we need to quench three conditions; Equilibrium, compatibility and the stress-strain law. This is attained by using finite elements by the application of principal of virtual work [1].

3.2 Finite Element Method:

Usually, for any structural analysis problem, stresses and displacements throughout the structure are determined. There are two general close in to find out stresses and displacements within a body using the finite element method. The flexibility method uses internal forces as the unbeknown of the problem to obtain the governing equations. A set of algebraic equations in terms of internal forces are then used for determining the redundant or unbeknown forces. These algebraic equations are combination of equilibrium equations and compatibility equations. The stiffness method on the other hand assumes that the displacements of the nodes are unbeknown and uses them in finding the governing equations. Algebraic equations are expressed in terms of nodal displacements exercising the equations of equilibrium and an applicable law relating forces to displacements [1].

When ductile metals are loaded beyond elastic range, the linear stress strain relation is taken over by complex nonlinear relation accompanied by much reduced of modulus as compared to modulus of elasticity. Finite element elastic-plastic analysis is much more complicated than simple elastic analysis. The Finite element method equation is not the same as for linear. It is substituted by a set of nonlinear equations that are to be solved by iteration. Iteration basically divides the total applied load into small increments for more accurate numerical results [1].

ANSYS (2007) is a software tool for solving a wide range variety of finite element problems. These problems contain static, dynamic structural analysis (linear or non-linear), heat transfer, fluid flow, mass transport, acoustic and electromagnetic problems. The analyst defines the finite element model properties such as position of the element nodal coordinates, the way in which elements are connected, material properties, applied loads, boundary conditions and the kind of analysis to be performed (ANSYS 2009) [1].

The flowchart in *Figure 3.1* shows the procedure of enhancing the model after every run until the desired results are obtained for basic model. Finite element modeling procedure starts by defining a case study with complete parameters. Different parameters of the model are determined and conditions are set. The preliminary model is solved for results and interpretation of these results defines the precision of the model. For any differences the model is refined and remodeled to get better results. This process continues until desired precision is obtained in the results [1].

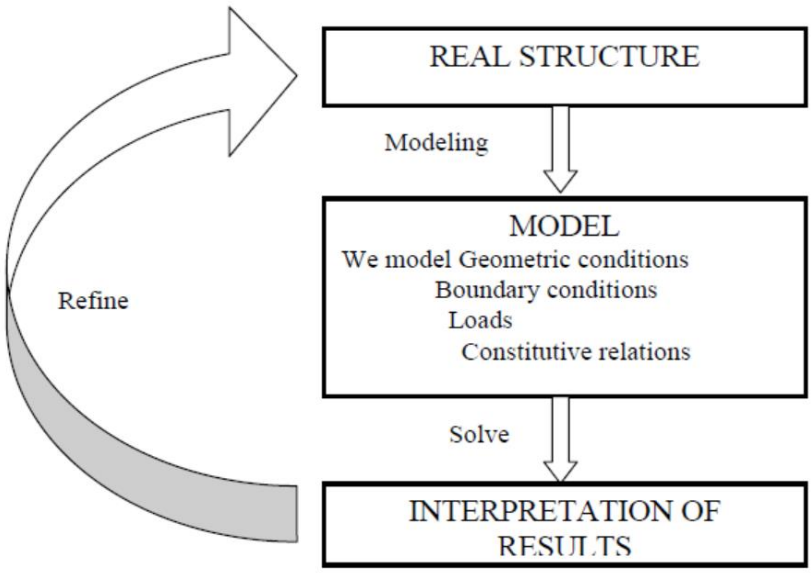

Fig. 3.1: Flow chart of analysis in using software tool [1].

3.3 Modeling Considerations

When an element is subjected to increasing loads, the stresses start increasing until it eventually gives out. It is comparatively simple to determine the point of failure of a component subject to a single tensile force. The strength data on the material identifies this particular strength. However, when the material is subject to a too many of loads in different directions some of which are tensile and some of which are shear, then the determination of the point of failure is more complicated [1].

Figure 3.2 shows that stress-strain curve assimilation between brittle and ductile materials, along with highly ductile fracture in which the specimen necks down to a point, moderately ductile failure after some necking, and brittle fracture without any plastic deformation [1].

Metals can be classified into ductile metals and brittle metals. Examples of ductile metals include mild steel and copper; on contrary, cast iron is a typical example of brittle metal. Ductile metals under high stress levels at first deform elastically at a definite yield point. After passing the yield point the material experiences eternal deformations. Prior to failure a ductile metal will have experienced a significant degree of elongation. In short, there is extensive plastic deformation and energy absorption (toughness) before fracture in

ductile metals. Ductile materials give out on planes of maximum shear stress. Ductility is the extent to which a material will deform before ultimate fracture. Percentage elongation is used to expedient ductility [1].

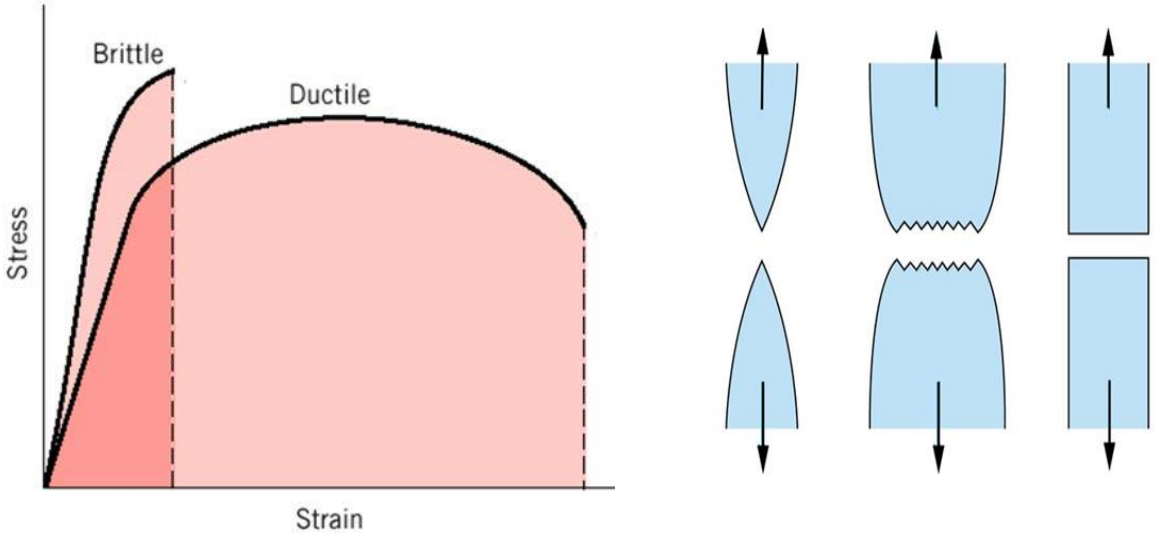

(a) σ−ε relation **(b)** high ductility **(c)** medium ductility **(d)** brittle

Fig.3.2: Ductile versus brittle behavior of materials [1].

In general, ductile materials experience more than 5% elongation at failure; whereas brittle materials do not have the capability to go through such a degree of deformation (Horne 1979). Brittle metals experience little ultimate elongation prior to failure and failure is generally sudden, without warning. There is low plastic deformation and low energy absorption before failure in brittle metals. Brittle materials often break on planes of maximum normal stress [1].

Structural steel is characterized by its capacity to withstand considerable deformation past first yield without fracture. When the load is applied to a steel specimen and is increased with time, initially the specimen behaves purely elastic. This means that the stress in every fiber is proportional to its strain and to its length from the neutral axis [1].

When the load is further increased after the stress in the extreme fibers reach the valuation of yield stress, then the extreme fibers yield at constant stress while the fibers near

to the neutral axis sustain increased elastic stresses. A zone of yielding (plastic zone) evolve at the first critical section. The moment at this section remains more or less constant due to ductility of steel and the load is transferred to less heavily stressed portions (Horne 1979). This causes new zones of yielding at other sections in the steel specimen until the maximum moment is reached at all critical zones. The plastic zones amplify in depth until they reach the neutral axis [15].

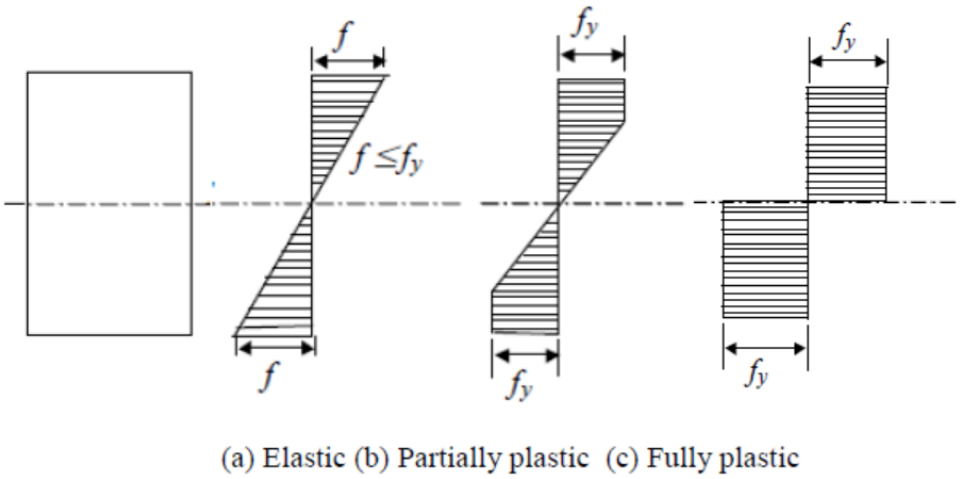

Fig. 3.3: Flexural stresses in steel cross-sections (Horne 1979) [1].

Beyond this point the structure would simply deform at constant load without any load proliferation and act as a hinge. This is referred to as plastic hinge and it transmits a constant moment. The bending moment producing a plastic hinge in the section is called the complete plastic moment. Stress distributions in a rectangular beam for elastic, partially plastic and fully plastic section are revealed below in the *Figure 3.3* [15].

Generally, codes (such as IS 800, BS 5950) allow use of plastic design only where loading is predominantly static and fatigue is not a design principle. BS 5950 defines the general requirements for utilizing plastic design concepts (Malik 1988). It says that, the yield plateau (horizontal portion of the curve) must be greater than 6 times the yield strain, the ultimate tensile strength must be more than 1.2 times the yield strength and the elongation on a standard gauge length should not be less than 15%. These limitations are intended to make sure that there is sufficiently huge plastic plateau to enable a hinge to form and that the steel will not experience a premature strain hardening [1].

Mesh size and type is also very significant factor in modeling considerations. Triangular or tetrahedral elements must not be used to evade rigid body motion in the model. Square shaped or else rectangular elements are favoured for finite element analysis. For high accuracy, the width to length ratio (aspect ratio) of any element should not exceed 1.5 (Nelson and Wang 2006) [1].

The appropriate mesh size for any object can be determined by plotting nodal stresses along to each line in the mesh. This benefits in identifying the stress jump at any point where more than one element connects together. However, it will be very dynamic task to check stress jump along each line in the mesh of thousand lines. An alternative option is to use pressure bands which can show stress disjointedness. In case of inferior mesh size there will be stress disjointedness along the pressure band line. The stress disjointedness is represented by breaks in pressure bands. As the mesh is refined, the pressure bands gets smoother. Smooth pressure bands indicate that the stresses are smooth within the object and the mesh is acceptable (Bathe 1982) [1].

The degree of refinement of the mesh actually depends on the nature of the analysis being performed. In case of linearly elastic analysis, coarse mesh is adequate to calculate displacements and stress intensity factors. However, to calculate stresses in linear elastic material analysis we need a fine mesh. For non-linear analysis there is always a fine mesh preferred because we need accurate stresses. Accurate stresses are required as we go through the time increments of load to determine exact yield point (Budgell 1999). Once the yield point is crossed the stresses will vary in a non-linear manner and accuracy is very important in determining them. Different mesh sizes were tried in ANSYS before selecting the most appropriate mesh matching the results of laboratory testing [1].

There are generally three types of nonlinearities in a structure. When considering either highly flexible components, or structural assemblies comprising multiple components, progressive displacement gives rise to the possibility of either self or component-to-component contact. This characterizes to a specific class of geometrically nonlinear effects known collectively as boundary condition or ‘contact’ nonlinearity. Structures whose stiffness is dependent on the displacement which they may undergo are termed as geometrically nonlinear. Geometric nonlinearity accounts for phenomena such as the stiffening of a loaded clamped plate, and buckling or 'snap-through' behavior in slender structures or components. Material nonlinearity refers to the ability of a material to exhibit

a nonlinear stress-strain response. Elasto-plastic, hyper elastic, crushing, and cracking are good examples, but this can also include temperature and time-dependent effects such as visco-elasticity or visco-plasticity (creep) [1].

There is a rule of thumb that if the out of plane deflection of a flat plate is greater than half the thickness, then membrane forces start to become significant in resisting the externally applied load (Budgell 1999). In ANSYS, this calls for activating large displacement solution (geometric non-linearity). Membrane stresses can affect the structure in gaining more strength or vice versa. If shell models of flat plates subjected to pressure or perpendicular forces are under study, then initially the shell will carry the applied load by bending. Membrane forces will begin to carry the applied load when the bending increases by half of the shell thickness [1].

When the applied forces and displacements vary slowly then the analysis is called a static analysis. This means that the frequencies of the loads are much smaller than the natural frequencies of the structure. Transient analysis is in which load is applied and removed or applied in both directions. We will consider a static analysis stress-strain curve studied beyond 6 times the yield strain according to BS 5950 (1988) [1].

3.4 Work Plan

The methodology followed to achieve the stated objectives:

Task 1: Literature Review.

Task 2: Finite Element Method.

Task 3: Load Calculations.

Task 4: Detailed FEM analysis of models using ANSYS software.

Task 5: Analysis of the Results

Task 6: Recommendations and Conclusions

A brief description of the required work in each task are as follows:

Task 1: Literature Review

The research activities require a thorough literature review to understand the problem and be familiar with published work, so that previous research will not be duplicated. From the literature survey all the objectives got clear.

Task 2: Finite Element Method

Information on appropriate finite element modeling procedures for steel base plates was gathered to obtain appropriate results from the software. Finite element method has to be clearly understood and previous work in the area was studied.

Task 3: Load Calculations

Table 3.1 shows load calculations where K_1 is probability factor, K_2 is terrain, height and structure size factor, K_3 is topography factor and V_z is design wind speed at height z.

Dead Load	15 KN (Referred from "Non-Linear finite element analysis of steel base plate on leveling nuts By Abdul Wahab Kayani"[1]
Live Load (As per IS 875: Part-3)	K_1=1, K_2=1.05, K_3=1, V_z=47 m/sec (For Delhi) [From: Table-1,2 and Cl- 5.3.3.1, Cl- 5.3.3.2]
	$\text{Design Wind Speed } (P_Z) = 0.6 \times V_Z^2 \times (K_1 \times K_2 \times K_3)^2$ $= 0.6 \times 47^2 \times (1 \times 1.05 \times 1)^2$ $= 1461.25\ \text{N/m}^2$
	$\text{Wind Force on Face of Column}(F) = (C_{pe} - C_{pi}) \times A \times P_Z$ $= (0.8 - 0) \times 0.7 \times 0.2 \times 1461.25$ $= 163.66\ \text{N}$ $\frac{\text{Force}}{\text{Area}} = 0.001167\text{N/mm}^2$

Table-3.1: Load Calculations [22], [23].

Task 4: Detailed FEM analysis of models using ANSYS software

This task involves a thorough analysis of base plate using ANSYS. Several parameters were varied to study the structural behavior of the base plate. Material nonlinearity was taken into account. Square and circular plates ranging from 5mm thickness to 18mm thickness were used. The base plate had 4 or 8 anchor bolts, located at different spacing between them and distance from the face of the column. The plan dimensions of the base plate were 500mm×500mm for square plate and 564.189mm diameter for circular plate. The steel material was modeled as elastic-perfectly plastic with yield strength equal to 250MPa. The applied loading consisted of either concentric or eccentric vertical load, resulting in uniform compression, uniaxial bending, or biaxial bending stresses within the plate. Various steps involved in FEM analysis using ANSYS software were:

STEP-1 Creating of geometry:

Various geometries for square plate and circular plates were created as shown in *Fig. 3.4* and *Fig. 3.5*. These plates vary from 5mm thickness to 18mm thickness. Number of bolts used were 4. These bolts were placed at an eccentricity of 75 form edge of plate. The size of column used was 200×200 mm in which steel column created was of 8mm thickness inside which is a 186×186 mm concrete column is placed. The height of column is taken as 700mm [25].

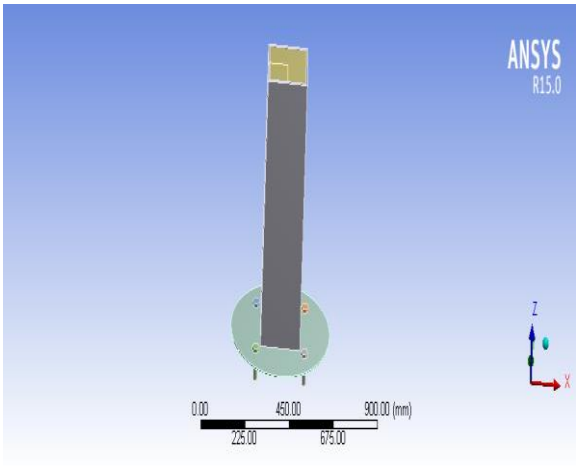

Fig. 3.4- Geometry of Circular Base Plate [24].

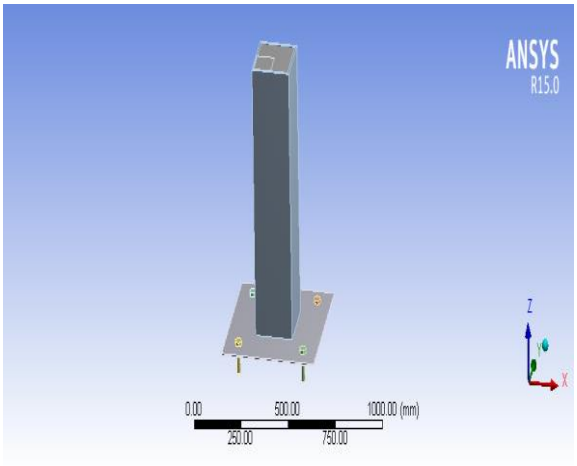

Fig. 3.5- Geometry of Square Base Plate [24].

STEP-2 Meshing:

Before selecting the mesh size, a convergence study was conducted which is shown in *Fig. 3.6*. In this study a graph was plotted between total deformation in case of square plate of 5mm thickness with 4 anchor rods and different mesh size. It can be seen clearly form *Fig. 3.6* that there not much significant change in deformation when the mesh size is taken to be 10mm and below. Therefore, 10 mm mesh was used as shown in *Fig. 3.7*.

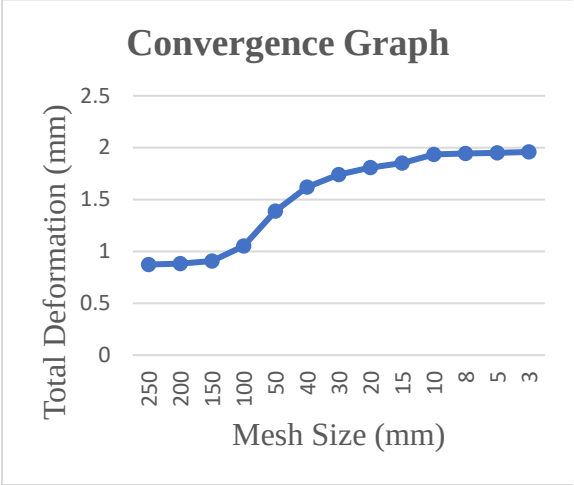

Fig. 3.6- Convergence Graph.

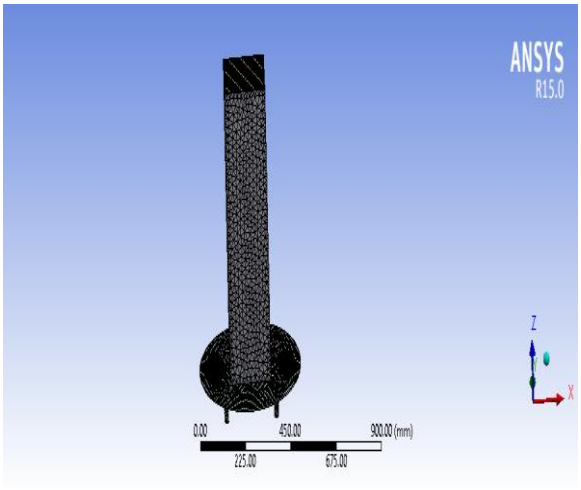

Fig. 3.7- Meshed geometry [24].

STEP-3 Boundary Conditions:

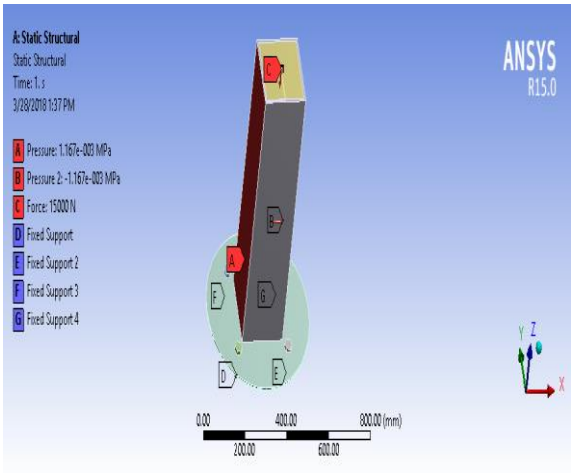

Fig. 3.8- Concentric Loading [24].

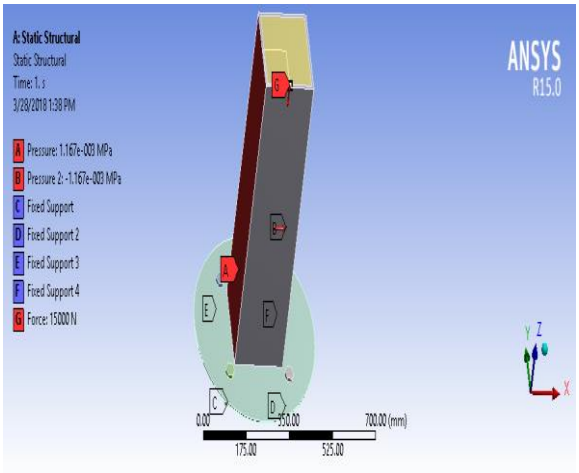

Fig. 3.9- Uniaxial Loading [24].

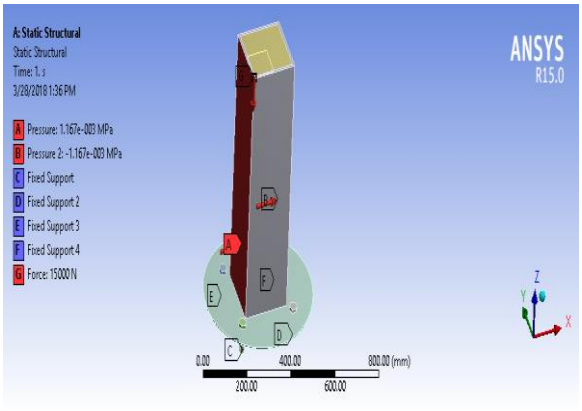

Fig. 3.10- Biaxial Loading [24].

All 4 bolts were assigned with fixed supports, also the column was assigned with 0.001167 N/mm^2 of wind load and a point load of 15KN was assigned at three locations i.e. Concentrically, Uniaxially, Biaxially as shown in *Fig. 3.8, 3.9, 3.10* respectively.

STEP-4 Types of Elements used:

The type of element used were program controlled. ANSYS software used 5 types of element while analyzing the 5mm thick plate and are shown in *Fig.-3.11*. These 5 types of element which were used are:

1. SOLID 186 elements.
2. SOLID 187 elements.
3. CONTA 174 element.
4. TARGE 170 element.
5. CLOAD 201 element.

*** ELEMENT RESULT CALCULATION TIMES

TYPE	NUMBER	ENAME	TOTAL CP	AVE CP
1	8554	SOLID186	3.203	0.000374
2	5737	SOLID187	0.984	0.000172
3	175	SOLID187	0.031	0.000179
4	170	SOLID187	0.062	0.000368
5	181	SOLID187	0.031	0.000173
6	175	SOLID187	0.031	0.000179
7	1195	SOLID186	0.438	0.000366
8	4196	CONTA174	0.422	0.000101
9	4196	TARGE170	0.109	0.000026
10	380	CONTA174	0.062	0.000164
11	380	TARGE170	0.000	0.000000
12	240	CONTA174	0.016	0.000065
13	240	TARGE170	0.000	0.000000
14	64	CONTA174	0.016	0.000244
15	64	TARGE170	0.000	0.000000
16	67	CONTA174	0.000	0.000000
17	67	TARGE170	0.000	0.000000
18	67	CONTA174	0.000	0.000000
19	67	TARGE170	0.000	0.000000
20	68	CONTA174	0.000	0.000000
21	68	TARGE170	0.000	0.000000
22	3	CLOAD201	0.000	0.000000

*** NODAL LOAD CALCULATION TIMES

TYPE	NUMBER	ENAME	TOTAL CP	AVE CP

Fig. 3.11: Types of Elements [24].

Task 6: Analysis of the Results

The results obtained by the detailed parametric studies were tabulated and analyzed. The finite element method was used to determine the total deformation, equivalent elastic strain, maximum principal elastic strain, minimum principal elastic strain, maximum elastic shear strain, equivalent stress, maximum principal stress, minimum principal stress and maximum shear stress in both the square base plate and circular base plate.

Task 7: Recommendations and Conclusions

The various results obtained from ANSYS software will be compared for square base plate and circular base plate of different thicknesses.

CHAPTER 4

RESULTS AND DISCUSSIONS

4.1 Graphical Comparison of Square and Circular Base Plate:

4.1.1 For Concentric Loading (4 anchor rods):

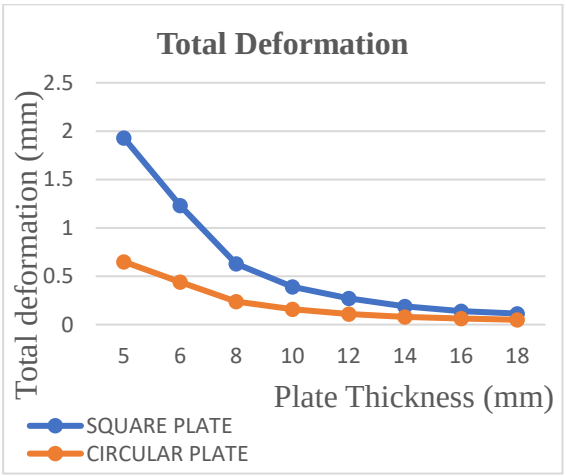

Fig. 4.1: Effect of Plate Geometry on Total Deformation (Concentric loading with 4 anchor rods).

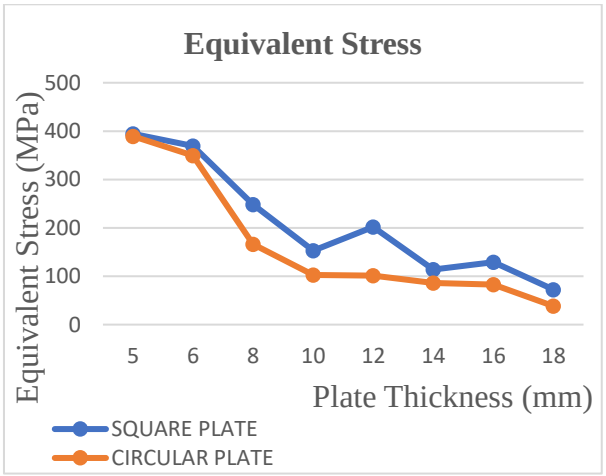

Fig. 4.2: Effect of Plate Geometry on Equivalent stress (Concentric loading with 4 anchor rods).

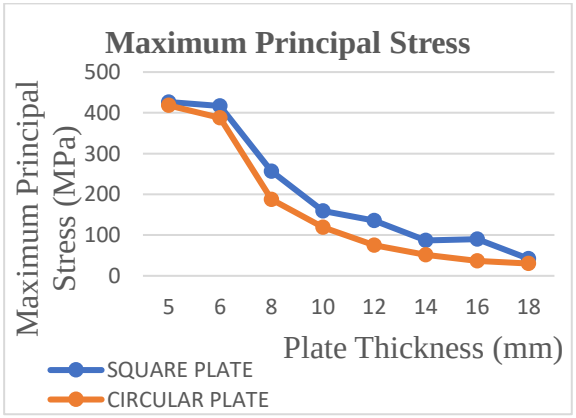

Fig. 4.3: Effect of Plate Geometry on Maximum Principal Stress (Concentric loading with 4 anchor rods).

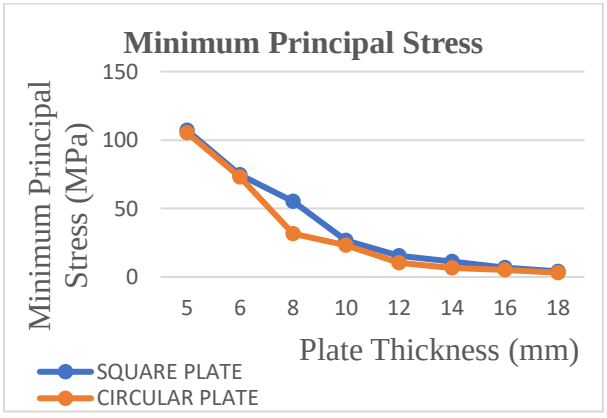

Fig. 4.4: Effect of Plate Geometry on Minimum Principal Stress (Concentric loading with 4 anchor rods).

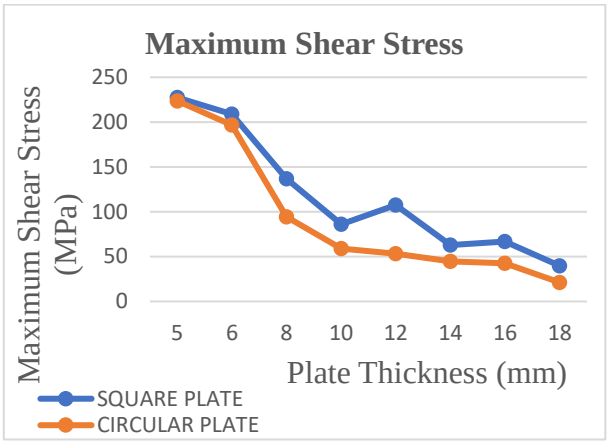

Fig. 4.5: Effect of Plate Geometry on Maximum Shear Stress (Concentric loading with 4 anchor rods).

From *Fig. 4.1* it can be seen that as the thickness of the plate increases the total deformation of the plate decreases. However, it is also clear from *Fig. 4.1* that the total deformation in case of circular plate is significantly lesser in case of square plate at lower thicknesses. Also, as the thickness of plate increases the graph between square plate and circular plate converges and there is no significant change in total deformation at higher thickness of 18mm.

From *Fig. 4.2* it can be seen that as the thickness of the plate increases the equivalent stress of the plate decreases (both square and circular). But for square plate the equivalent stress decreases up to 10mm thickness after which there is a slight increase in equivalent stress for 12 mm thickness and again it decreases up to 18mm thickness. However, the equivalent stress in case of square plate is significantly higher than in case of circular plate at almost all thicknesses except in case of 5mm thickness.

From *Fig. 4.3* it can be seen that as the thickness of the plate increases the maximum principal stress of the plate decreases. However, the maximum principal stress in case of square plate is significantly higher than in case of circular plate at almost all thicknesses except for 5mm and 18mm thicknesses.

From *Fig. 4.4* it can be seen that as the thickness of the plate increases the minimum principal stress of the plate decreases. However, the minimum principal stress in case of square plate is significantly higher than in case of circular plate at almost all thicknesses except for 5mm, 6mm, 16mm and 18mm thicknesses.

From *Fig. 4.5* it can be seen that as the thickness of the plate increases the maximum shear stress of the plate decreases (both square and circular). But for square plate the equivalent stress decreases up to 10mm thickness after which there is a slight increase in maximum shear stress for 12 mm thickness and again it decreases up to 18mm thickness. However, the maximum shear stress in case of square plate is significantly higher than in case of circular plate at almost all thicknesses except for 5mm thickness.

4.1.2 For Concentric Loading (8 anchor rods):

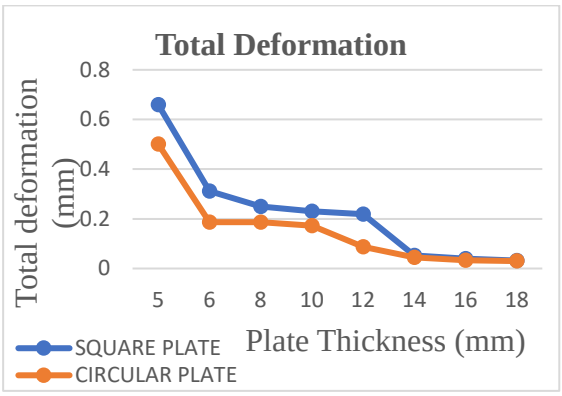

Fig. 4.6: Effect of Plate Geometry on Total Deformation (Concentric loading with 8 anchor rods).

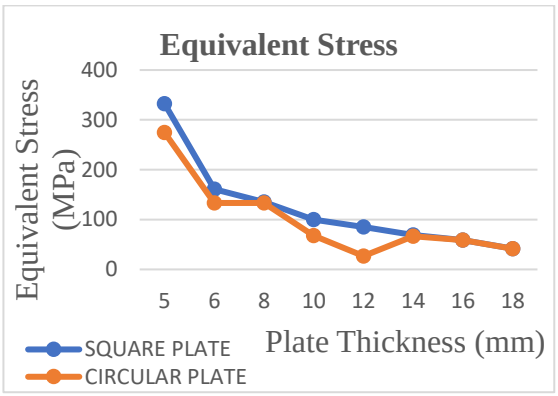

Fig. 4.7: Effect of Plate Geometry on Equivalent stress (Concentric loading with 8 anchor rods).

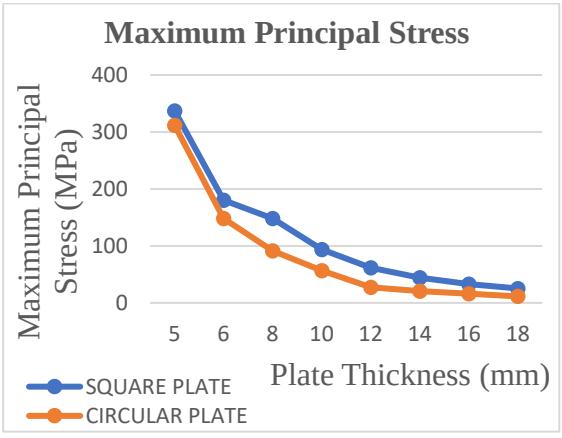

Fig. 4.8: Effect of Plate Geometry on Maximum Principal Stress (Concentric loading with 8 anchor rods).

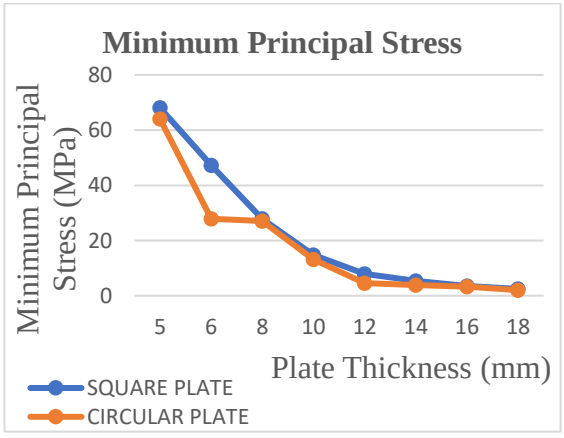

Fig. 4.9: Effect of Plate Geometry on Minimum Principal Stress (Concentric loading with 8 anchor rods).

Fig. 4.10: Effect of Plate Geometry on Maximum Shear Stress (Concentric loading with 8 anchor rods).

From *Fig. 4.6* it can be seen that as the thickness of the plate increases the total deformation of the plate decreases. However, it is also clear from *Fig. 4.6* that the total deformation in case of circular plate is significantly lesser in case of square plate at almost all thicknesses except for 14mm, 16mm and 18mm thicknesses.

From *Fig. 4.7* it can be seen that as the thickness of the plate increases the equivalent stress of the plate decreases (both square and circular). But for circular plate the equivalent stress decreases up to 6mm thickness after which there is a slight increase in equivalent stress for 8mm thickness and again it decreases up to 12mm thickness after which there is again a slight increase in equivalent stress up to 14mm thickness and then decreases up to 18mm thickness. However, the equivalent stress in case of square plate is significantly higher than in case of circular plate at almost all thicknesses except in case of 8mm, 14mm, 16mm and 18mm thicknesses.

From *Fig. 4.8* it can be seen that as the thickness of the plate increases the maximum principal stress of the plate decreases. However, the maximum principal stress in case of square plate is significantly higher than in case of circular plate for all thicknesses.

From *Fig. 4.9* it can be seen that as the thickness of the plate increases the minimum principal stress of the plate decreases. However, the minimum principal stress in case of square plate is significantly higher than in case of circular plate at almost all thicknesses except for 5mm, 6mm, 16mm and 18mm thicknesses.

From *Fig. 4.10* it can be seen that as the thickness of the plate increases the maximum shear stress of the plate decreases. However, the maximum shear stress in case of square plate is significantly higher than in case of circular plate at almost all thicknesses except for 5mm thickness.

4.1.3 For Uniaxial Loading (4 anchor rods):

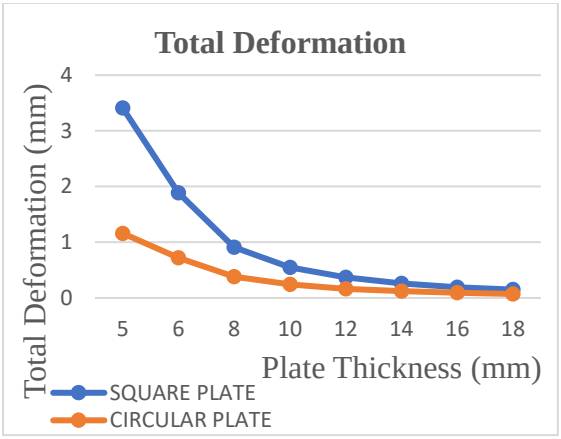

Fig. 4.11: Effect of Plate Geometry on Total Deformation (Uniaxial loading with 4 anchor rods).

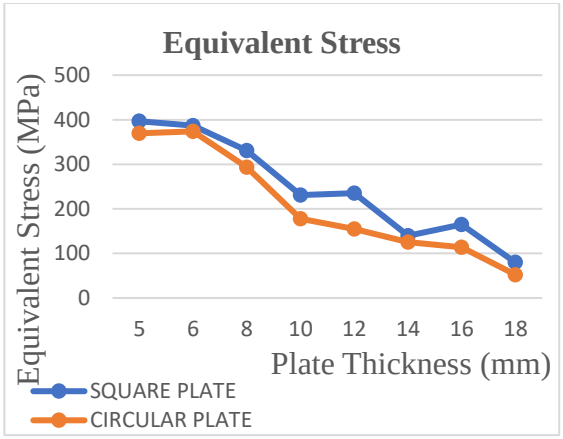

Fig. 4.12: Effect of Plate Geometry on Equivalent Stress (Uniaxial loading with 4 anchor rods).

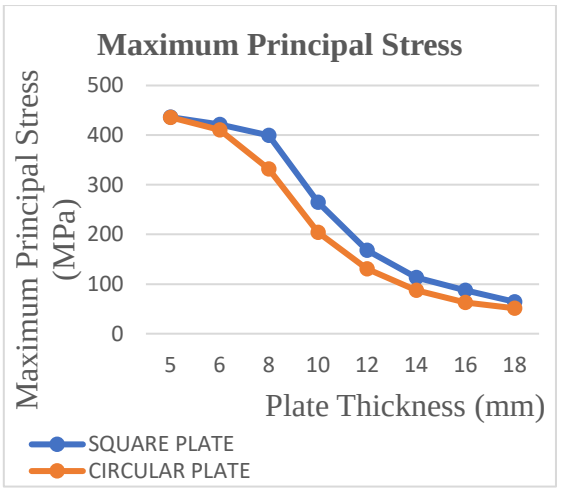

Fig. 4.13: Effect of Plate Geometry on Maximum Principal Stress (Uniaxial loading with 4 anchor rods).

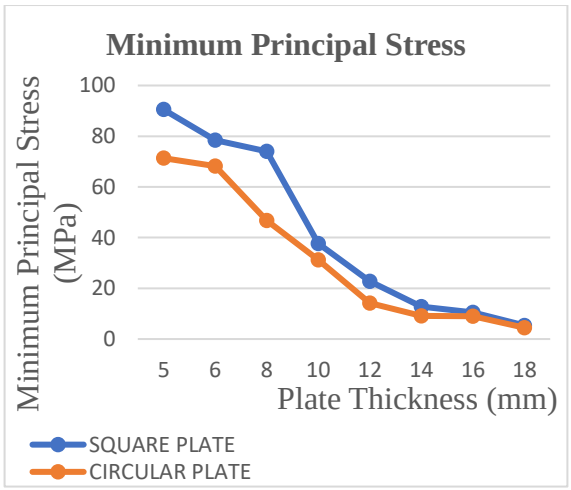

Fig. 4.14: Effect of Plate Geometry on Minimum Principal Stress (Uniaxial loading with 4 anchor rods).

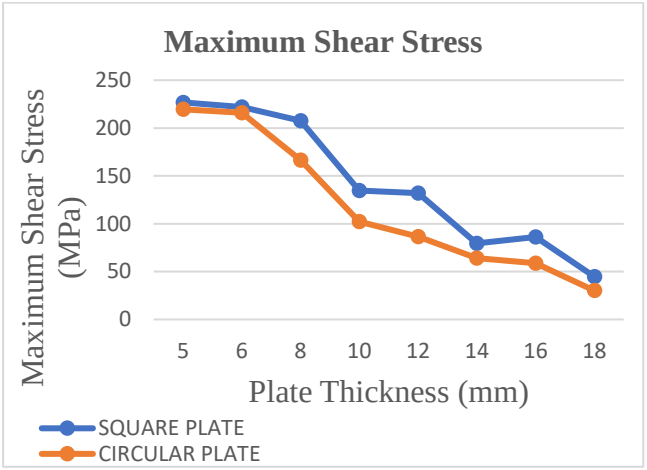

Fig. 4.15: Effect of Plate Geometry on Maximum Shear Stress (Uniaxial loading with 4 anchor rods).

From *Fig. 4.11* it can be seen that as the thickness of the plate increases the total deformation of the plate decreases. However, it is also clear from *Fig. 4.11* that the total deformation in case of circular plate is significantly lesser in case of square plate at lower thicknesses. Also, as the thickness of plate increases the graph between square plate and circular plate converges and there is no significant change in total deformation at higher thickness of 18mm.

From *Fig. 4.12* it can be seen that as the thickness of the plate increases the equivalent stress of the plate decreases (both square and circular). But for square plate the equivalent stress decreases up to 10mm thickness after which there is a slight increase in equivalent stress for 12mm thickness and again it decreases up to 14mm thickness after which there is again a slight increase in equivalent stress up to 16mm thickness and then decreases up to 18mm thickness. However, the equivalent stress in case of square plate is significantly higher than in case of circular plate at almost all thicknesses except in case of 6mm and 14mm thicknesses.

From *Fig. 4.13* it can be seen that as the thickness of the plate increases the maximum principal stress of the plate decreases. However, the maximum principal stress in case of square plate is significantly higher than in case of circular plate for almost all thicknesses except for 5mm, 6mm and 18mm thicknesses.

From *Fig. 4.14* it can be seen that as the thickness of the plate increases the minimum principal stress of the plate decreases. However, the minimum principal stress in case of square plate is significantly higher than in case of circular plate at almost all thicknesses except for 16mm and 18mm thicknesses.

From *Fig. 4.15* it can be seen that as the thickness of the plate increases the maximum shear stress of the plate decreases (both square and circular). But for square plate the maximum shear stress decreases up to 10mm thickness after which there is a slight increase in maximum shear stress for 12 mm thickness and again it decreases up to 14mm and increases up to 16mm and then again decreases up to 18mm thickness. However, the maximum shear stress in case of square plate is significantly higher than in case of circular plate at almost all thicknesses except in case of 5mm thickness.

4.1.4 For Uniaxial Loading (8 anchor rods):

From *Fig. 4.16* it can be seen that as the thickness of the plate increases the total deformation of the plate decreases. However, it is also clear from *Fig. 4.16* that the total deformation in case of circular plate is significantly lesser in case of square plate at lower thicknesses. Also, as the thickness of plate increases the graph between square plate and circular plate converges and there is no significant change in total deformation at higher thicknesses of 14mm, 16mm and 18mm.

From *Fig. 4.17* it can be seen that as the thickness of the plate increases the equivalent stress of the plate decreases. However, the equivalent stress in case of square plate is significantly higher than in case of circular plate at almost all thicknesses except for 12mm, 14mm and 16mm thicknesses.

From *Fig. 4.18* it can be seen that as the thickness of the plate increases the maximum principal stress of the plate decreases. However, the maximum principal stress in case of square plate is significantly higher than in case of circular plate for all thicknesses.

From *Fig. 4.19* it can be seen that as the thickness of the plate increases the minimum principal stress of the plate decreases. However, the minimum principal stress in case of square plate is significantly higher than in case of circular plate at almost all thicknesses except for 10mm, 12mm, 16mm and 18mm thicknesses.

From *Fig. 4.20* it can be seen that as the thickness of the plate increases the maximum shear stress of the plate decreases. However, the maximum shear stress in case of square plate is significantly higher than in case of circular plate for all thicknesses.

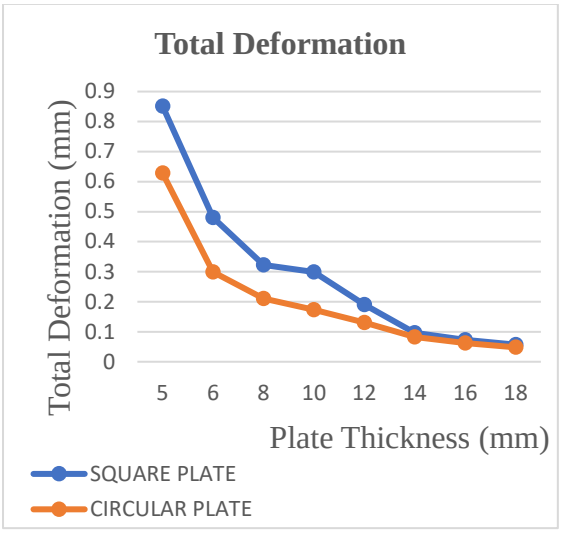

Fig. 4.16: Effect of Plate Geometry on Total Deformation (Uniaxial loading with 8 anchor rods).

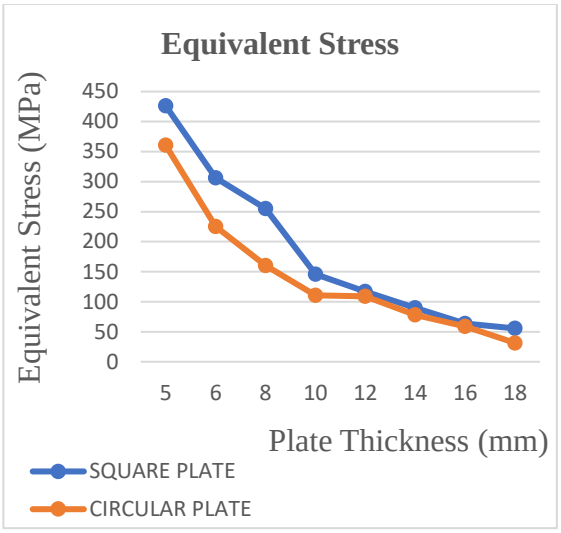

Fig. 4.17: Effect of Plate Geometry on Equivalent Stress (Uniaxial loading with 8 anchor rods).

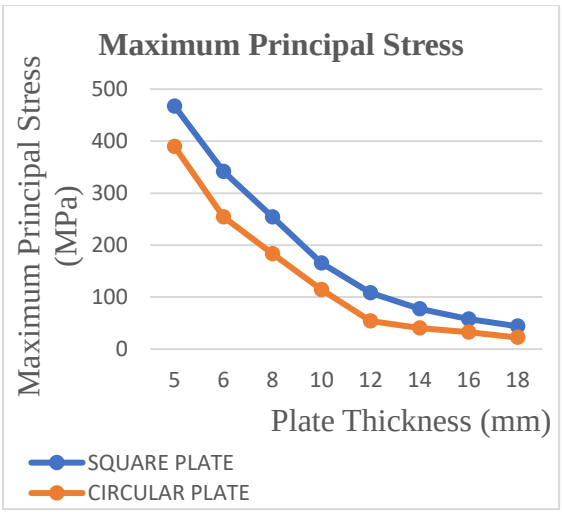

Fig. 4.18: Effect of Plate Geometry on Maximum Principal Stress (Uniaxial loading with 8 anchor rods).

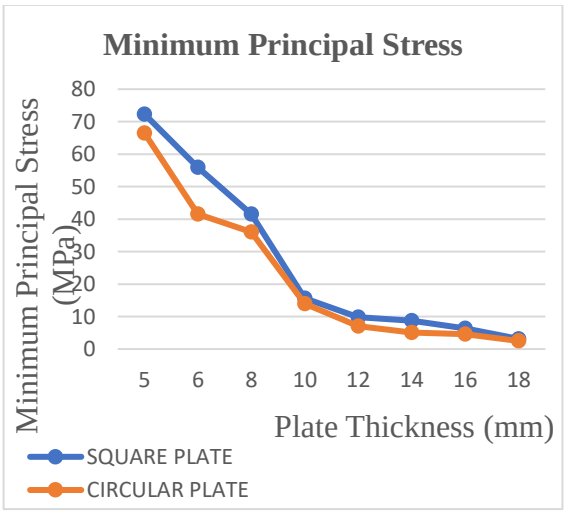

Fig. 4.19: Effect of Plate Geometry on Minimum Principal Stress (Uniaxial loading with 8 anchor rods).

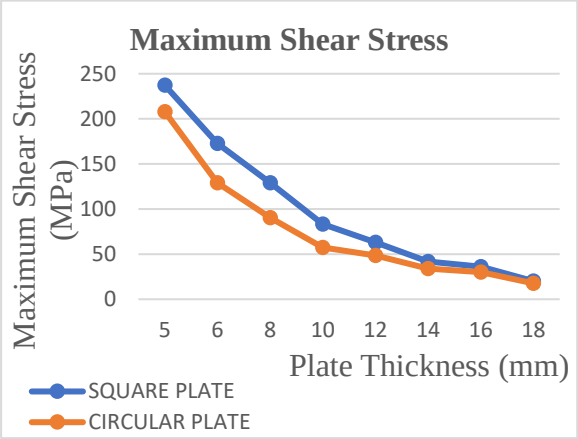

Fig. 4.20: Effect of Plate Geometry on Maximum Shear Stress (Uniaxial loading with 8 anchor rods).

4.1.5 For Biaxial Loading (4 anchor rods):

From *Fig. 4.21* it can be seen that as the thickness of the plate increases the total deformation of the plate decreases. However, it is also clear from *Fig. 4.21* that the total deformation in case of circular plate is significantly lesser in case of square plate at lower thicknesses. Also, as the thickness of plate increases the graph between square plate and circular plate converges and there is no significant change in total deformation at higher thickness of 18mm.

From *Fig. 4.22* it can be seen that as the thickness of the plate increases the equivalent stress of the plate decreases. However, the equivalent stress in case of square plate is significantly higher than in case of circular plate at almost all thicknesses except for 6mm thickness.

From *Fig. 4.23* it can be seen that as the thickness of the plate increases the maximum principal stress of the plate decreases. However, the maximum principal stress in case of square plate is significantly higher than in case of circular plate at almost all thicknesses except for 5mm, and 8mm thicknesses.

From *Fig. 4.24* it can be seen that as the thickness of the plate increases the minimum principal stress of the plate decreases. However, the minimum principal stress in case of

square plate is significantly higher than in case of circular plate at almost all thicknesses except for 14mm, 16mm and 18mm thicknesses.

From *Fig. 4.25* it can be seen that as the thickness of the plate increases the maximum shear stress of the plate decreases. However, the maximum shear stress in case of square plate is significantly higher than in case of circular plate for almost all thicknesses except for 6mm thickness.

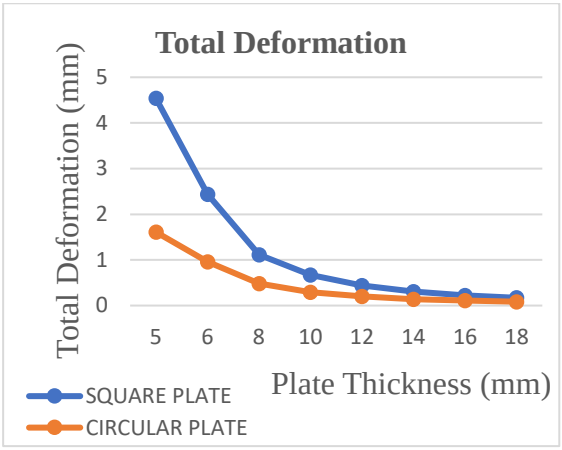

Fig. 4.21: Effect of Plate Geometry on Total Deformation (Biaxial loading with 4 anchor rods).

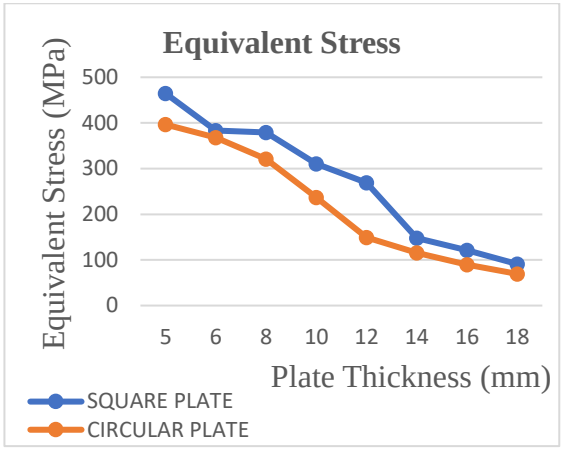

Fig. 4.22: Effect of Plate Geometry on Equivalent Stress (Biaxial loading with 4 anchor rods).

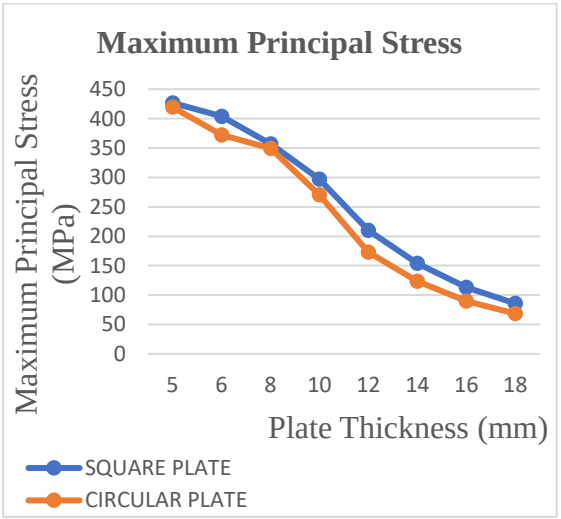

Fig. 4.23: Effect of Plate Geometry on Maximum Principal Stress (Biaxial loading with 4 anchor rods).

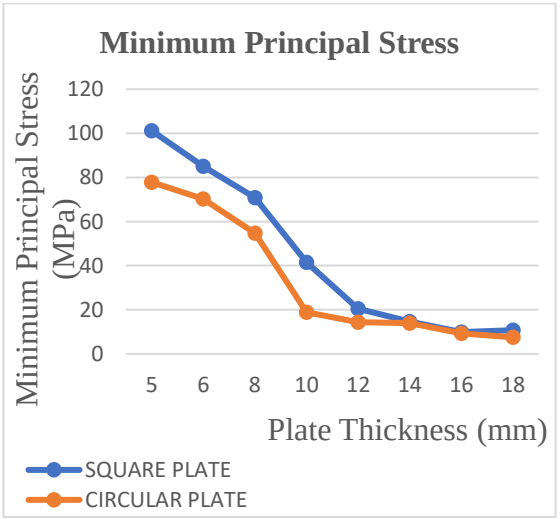

Fig. 4.24: Effect of Plate Geometry on Minimum Principal Stress (Biaxial loading with 4 anchor rods).

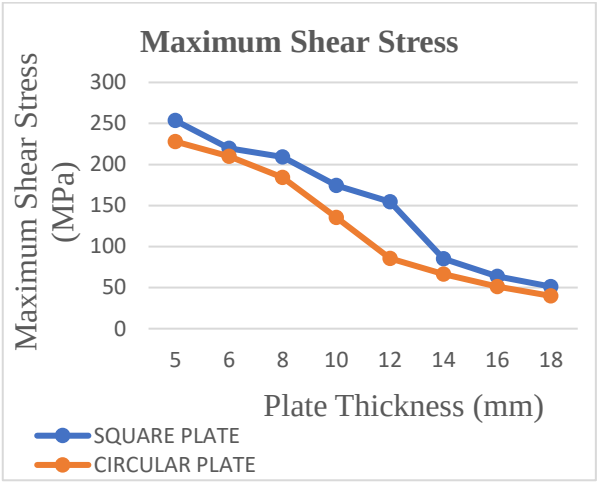

Fig. 4.25: Effect of Plate Geometry on Maximum Shear Stress (Biaxial loading with 4 anchor rods).

4.1.6 For Biaxial Loading (8 anchor rods):

From *Fig. 4.26* it can be seen that as the thickness of the plate increases the total deformation of the plate decreases. However, it is also clear from *Fig. 4.26* that the total deformation in case of circular plate is significantly lesser in case of square plate at lower thicknesses. Also, as the thickness of plate increases the graph between square plate and circular plate converges and there is no significant change in total deformation at higher thicknesses of 10mm, 12mm, 14mm, 16mm and 18mm.

From *Fig. 4.27* it can be seen that as the thickness of the plate increases the equivalent stress of the plate decreases. However, the equivalent stress in case of square plate is significantly higher than in case of circular plate at almost all thicknesses except for 14mm, 16mm and 18mm thicknesses.

From *Fig. 4.28* it can be seen that as the thickness of the plate increases the maximum principal stress of the plate decreases. However, the maximum principal stress in case of square plate is significantly higher than in case of circular plate at almost all thicknesses except for 6mm, and 16mm thicknesses.

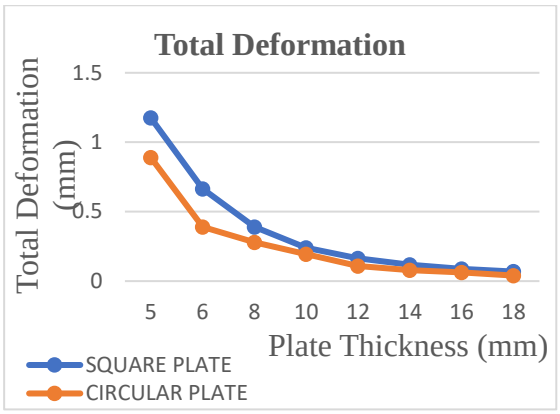

Fig. 4.26: Effect of Plate Geometry on Total Deformation (Biaxial loading with 8 anchor rods).

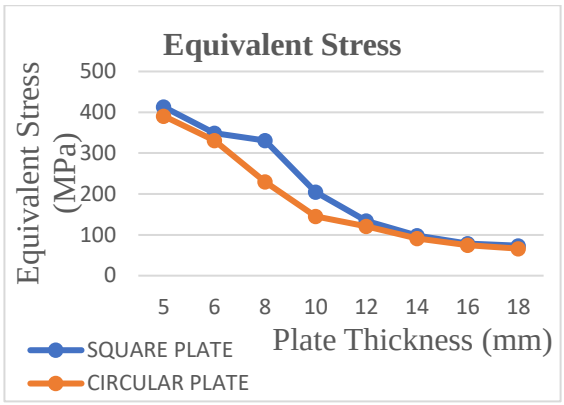

Fig. 4.27: Effect of Plate Geometry on Equivalent Stress (Biaxial loading with 8 anchor rods).

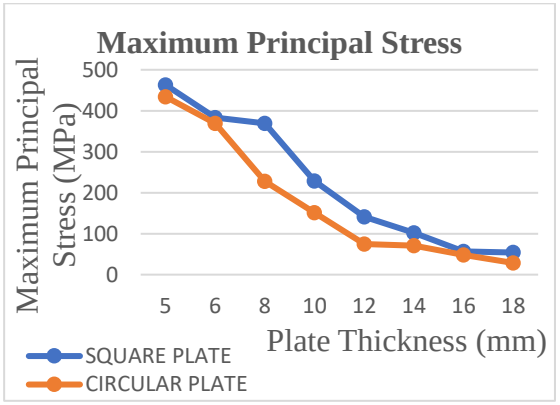

Fig. 4.28: Effect of Plate Geometry on Maximum Principal Stress (Biaxial loading with 8 anchor rods).

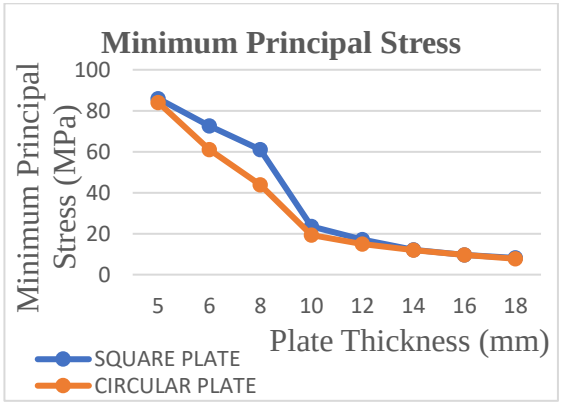

Fig. 4.29: Effect of Plate Geometry on Minimum Principal Stress (Biaxial loading with 8 anchor rods).

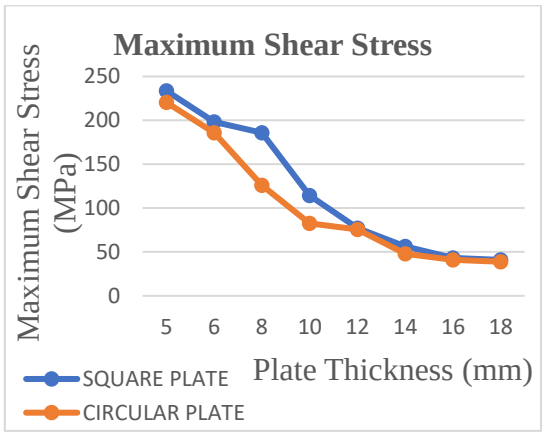

Fig. 4.30: Effect of Plate Geometry on Maximum Shear Stress (Biaxial loading with 8 anchor rods).

From *Fig. 4.29* it can be seen that as the thickness of the plate increases the minimum principal stress of the plate decreases. However, the minimum principal stress in case of square plate is significantly higher than in case of circular plate at almost all thicknesses except for 5mm, 12mm, 14mm, 16mm and 18mm thicknesses.

From *Fig. 4.30* it can be seen that as the thickness of the plate increases the maximum shear stress of the plate decreases. However, the maximum shear stress in case of square plate is significantly higher than in case of circular plate for almost all thicknesses except for 12mm, 16mm and 18mm thicknesses.

CHAPTER 5

CONCLUSIONS

5.1 Conclusions:

The results of the study lead to following important conclusions:

1. The various results calculated such as total deformation, equivalent stress, maximum principal stress, minimum principal stress and maximum shear stress were better when 8 anchor rods were used rather than when 4 anchor rods were used. However, when comparison between square and circular plate was made the number of anchor rod used didn't had much significance as circular plate gave better results for both 4 and 8 anchor rods respectively.
2. The nature of loading (concentric, uniaxial and biaxial) had no significant effect on the various results which were calculated.
3. The geometry of plate (square and circular) had visible difference on almost all the results calculated. Further it could be seen that circular plate gave better results than square plate on application of similar loading and also with similar area of plate.
4. The base plate of higher thickness gave better results (for both circular and square plates), but at the same time the economic factor was not taken into account.

5.2 Future Scope for Research:

Work can further be carried out for the wide flange column and hexagonal column instead of square and circular column used for analysis. Also, the economic factor can be taken into account when it comes to use of various thickness of base plate for analysis. When anchor rod distribution comes into account the use of unsymmetrical anchor rod distribution can be used for study. Also, in place of static loading (concentric, uniaxial and biaxial) effect, dynamic loading effect can be taken into account for analysis.

REFRENCES

[1] Kayani, A. W. (2012). "*Non-Linear Finite Element Analysis of Steel Base Plates on Leveling Nuts"* (Doctoral dissertation).

[2] Hamizi, M., & Hannachi, N. E. (2007). "Evaluation by a finite element method of the flexibility factor and fixity degree for the base plate connections commonly used", *Strength of Materials*, *39*(6), 588-599.

[3] Azzam, D., & Menzemer, C. C. (2006). "Fatigue behavior of welded aluminum light pole support details", *Journal of Structural Engineering*, *132*(12), 1919-1927.

[4] Abdalla, K. M., & Chen, W. F. (2006). "Base plate design in steel structures: A new approach", *Journal of Structural Engineering*, *33*(5), 375-382.

[5] Garlich, M. J., Thorkildsen, E. T., & Engineers, C. (2005). "*Guidelines for the installation, inspection, maintenance and repair of structural supports for highway signs, luminaires, and traffic signals*" (No. FHWA-NHI-05-036). United States. Federal Highway Administration.

[6] Nelson, T., & Wang, E. (2004). "Reliable FE-Modeling with ANSYS", In *International ANSYS Conference* (p. 93).

[7] Spacone, E., and El-Tawil, S. (2004). "Nonlinear analysis of steel-concrete composite structures: State of the art", *Journal of Structural Engineering*, *130*(2), 159-168.

[8] Hag-Elsafi, O., Alampalli, S., and Owens, F. (2001). "New Procedure for Design of End Plates and Base Plates of Cantilevered Traffic Support Structures", *Journal of Structural Engineering*, *127*(10), 1153-1163.

[9] Chan, S. L. (2001). "Non-linear behavior and design of steel structures", *Journal of Constructional Steel Research*, *57*(12), 1217-1231.

[10] Liew, J. R., Chen, H., and Shanmugam, N. E. (2001). "Inelastic analysis of steel frames with composite beams", *Journal of Structural Engineering*, *127*(2), 194-202.

[11] Wald, F., Jaspart, J. P., & Brown, D. (2000). "Base plate in bending and anchor bolts in tension", *Journal of Constructional Steel Research*.

[12] Sebastian, W. M., and McConnel, R. E. (2000). "Nonlinear FE analysis of steel-concrete composite structures", *Journal of Structural Engineering*, *126*(6), 662-674.

[13] Drake, R. M., and Elkin, S. J. (1999). "Beam-Column Base Plate Design-LRFD Method",*Engineering Journal-American Institute of Construction, 36*, 29-38.

[14] Thevendran, V., Chen, S., Shanmugam, N. E., and Liew, J. R. (1999). "Nonlinear analysis of steel–concrete composite beams curved in plan", *Finite Elements in Analysis and Design*, *32*(3), 125-139.

[15] Stamatopoulos, G. N., and Ermopoulos, J. C. (1997). "Interaction curves for column base-plate connections", *Journal of Constructional Steel Research*, *44*(1-2), 69-89.

[16] Ermopoulos, J. C., and Stamatopoulos, G. N. (1996). "Mathematical modelling of column base plate connections", *Journal of constructional steel research*, *36*(2), 79-100.

[17] Najjar, S. R., and Burgess, I. W. (1996). "A nonlinear analysis for three-dimensional steel frames in fire conditions", *Engineering structures*, *18*(1), 77-89.

[18] Kruger, T. S., Van Rensburg, B. W. J., and Du Plessis, G. M. (1995). "Non-linear analysis of structural steel frames", *Journal of Constructional Steel Research*, *34*(2-3), 285-306.

[19] Wong, M. B., and Tin-Loi, F. (1990). "Analysis of frames involving geometrical and material nonlinearities", *Computers & structures*, *34*(4), 641-646.

[20] Thambiratnam, D. P., and Paramasivam, P. (1986). "Base plates under axial loads and moments", *Journal of Structural Engineering*, *112*(5), 1166-1181.

[21] Patel, K. V., and Chen, W. F. (1984). "Nonlinear analysis of steel moment connections", *Journal of Structural Engineering*, *110*(8), 1861-1874.

[22] IS 800: 2007, GENERAL CONSTRUCTION IN STEEL- CODE OF PRACTICE (third revision).

[23] IS 875 (part-3):1987, CODE OF PRACTICE FOR DESIGN LOADS (OTHER THAN EARTHQUAKE) FOR BUILDINGS AND STRUCTURES (second revision).

[24] ANSYS® Academic Research Mechanical, Release 15.0 [Computer software].

[25] SolidWorks [Computer software].

APPENDIX A

Report file of ANSYS for circular base plate of 18mm thickness with 8 anchor rods and concentric loading:

Project

First Saved	Sunday, April 15, 2018
Last Saved	Sunday, April 15, 2018
Product Version	15.0 Release
Save Project Before Solution	No
Save Project After Solution	No

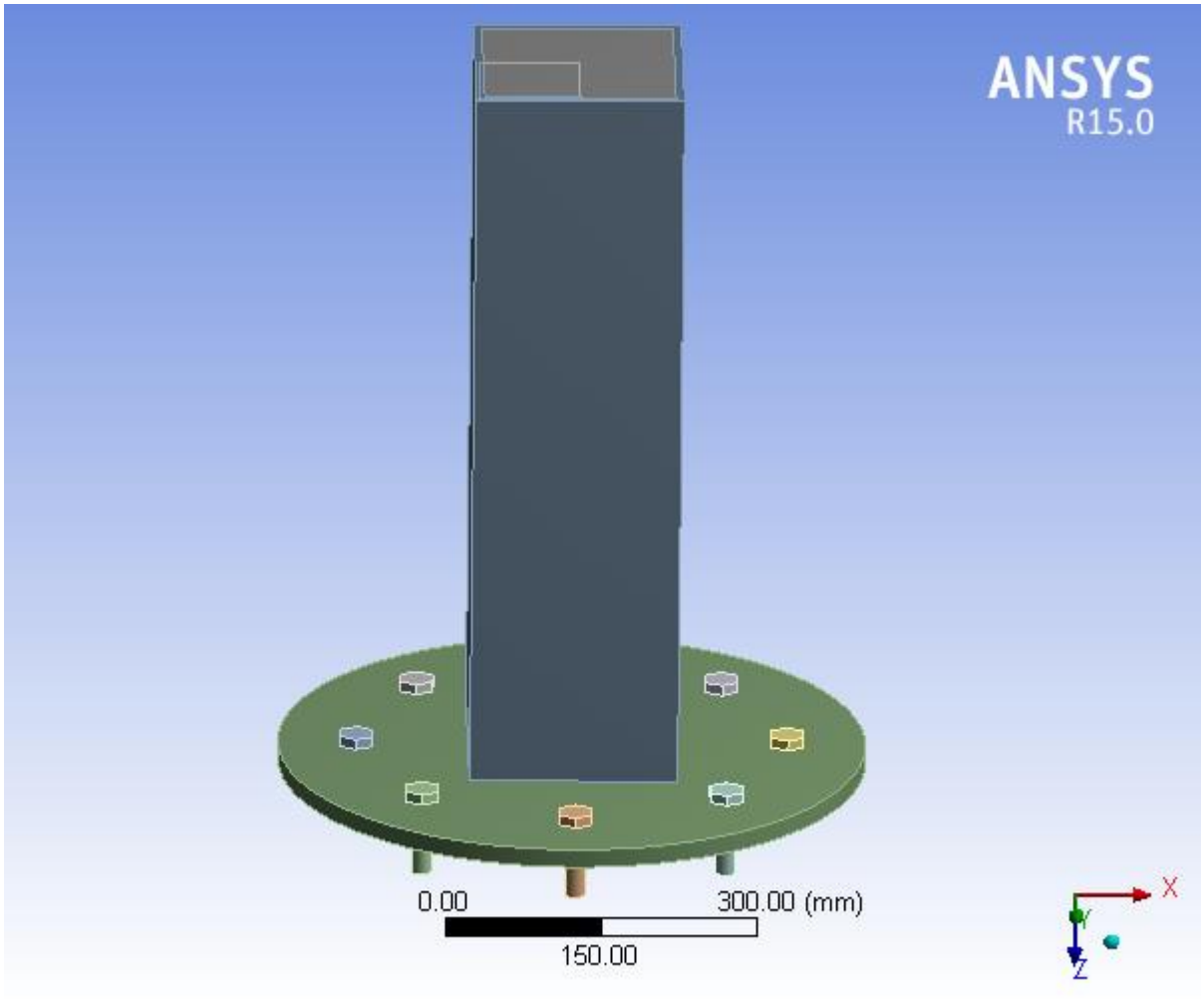

Fig. A: Assembly of column and circular base plate used for analyses.

Contents

Units

TABLE 1

Unit System	Metric (mm, t, N, s, mV, mA) Degrees rad/s Celsius
Angle	Degrees
Rotational Velocity	rad/s
Temperature	Celsius

Model (A4)

Geometry

TABLE 2
Model (A4) > Geometry

Object Name	*Geometry*
State	Fully Defined
Definition	
Source	C:\Users\user\Desktop\162656\Circular Plate\8 Bolts meshing and analysis\18mm\Concentric_files\dp0\SYS\DM\SYS.agdb
Type	DesignModeler

Length Unit	Meters
Element Control	Program Controlled
Display Style	Body Color
Bounding Box	
Length X	564.19 mm
Length Y	564.19 mm
Length Z	775. mm
Properties	
Volume	3.2696e+007 mm³
Mass	0.12514 t
Scale Factor Value	1.
Statistics	
Bodies	11
Active Bodies	11
Nodes	175836
Elements	45446
Mesh Metric	None
Basic Geometry Options	
Parameters	Yes
Parameter Key	DS
Attributes	No
Named Selections	No
Material Properties	No
Advanced Geometry Options	
Use Associativity	Yes
Coordinate Systems	No

Reader Mode Saves Updated File	No
Use Instances	Yes
Smart CAD Update	No
Compare Parts On Update	No
Attach File Via Temp File	Yes
Temporary Directory	C:\Users\user\AppData\Roaming\Ansys\v150
Analysis Type	3-D
Decompose Disjoint Geometry	Yes
Enclosure and Symmetry Processing	Yes

TABLE 3
Model (A4) > Geometry > Parts

Object Name	*Solid*	*Solid*	*Solid*	*Solid*	*Solid*	*Solid*	*Solid*	*Solid*	*Solid*	*Solid*	*Solid*
State	Meshed										
Graphics Properties											
Visible	Yes										
Transparency	1										
Definition											
Suppressed	No										
Stiffness Behavior	Flexible										
Coordinate System	Default Coordinate System										
Reference	By Environment										

Temperature										
Material										
Assignment	Structural Steel NL							Concrete NL	Structural Steel NL	
Nonlinear Effects	Yes									
Thermal Strain Effects	Yes									
Bounding Box										
Length X	32.288 mm		31.693 mm					184. mm	200. mm	564.19 mm
Length Y	36.003 mm		36.06 mm					184. mm	200. mm	564.19 mm
Length Z	85. mm							700. mm		18. mm
Properties										
Volume	29714 mm³							2.3699e+007 mm³	4.3008e+006 mm³	4.4587e+006 mm³
Mass	2.3325e-004 t							5.4508e-002 t	3.3761e-002 t	3.5001e-002 t
Centroid X	65.377 mm	4.7215 mm	65.377 mm	211.81 mm	358.25 mm	418.9 mm	358.25 mm	211.81 mm		
Centroid Y	218.43 mm	364.86 mm	511.3 mm	571.95 mm	511.3 mm	364.86 mm	218.43 mm	157.77 mm	364.86 mm	
Centroid Z	595.47 mm							220.09 mm		579.09 mm
Moment of Inertia Ip1	0.1724 t·mm²		0.17239 t·mm²					2379.5 t·mm²	1586.4 t·mm²	695.36 t·mm²
Moment of Inertia Ip2	0.1724 t·mm²	0.17241 t·mm²	0.17239 t·mm²					2379.5 t·mm²	1586.4 t·mm²	695.4 t·mm²

Moment of Inertia Ip3	1.6468e-002 t·mm²	1.6466e-002 t·mm²	307.57 t·mm²	415.58 t·mm²	1388.9 t·mm²
Statistics					
Nodes	450	448	115949	23152	33137
Elements	200	198	26600	11368	5880
Mesh Metric	None				

Coordinate Systems

TABLE 4
Model (A4) > Coordinate Systems > Coordinate System

Object Name	*Global Coordinate System*
State	Fully Defined
Definition	
Type	Cartesian
Coordinate System ID	0.
Origin	
Origin X	0. mm
Origin Y	0. mm
Origin Z	0. mm
Directional Vectors	
X Axis Data	[1. 0. 0.]
Y Axis Data	[0. 1. 0.]
Z Axis Data	[0. 0. 1.]

Connections

TABLE 5
Model (A4) > Connections

Object Name	*Connections*
State	Fully Defined

Auto Detection	
Generate Automatic Connection On Refresh	Yes
Transparency	
Enabled	Yes

TABLE 6
Model (A4) > Connections > Contacts

Object Name	*Contacts*
State	Fully Defined
Definition	
Connection Type	Contact
Scope	
Scoping Method	Geometry Selection
Geometry	All Bodies
Auto Detection	
Tolerance Type	Slider
Tolerance Slider	0.
Tolerance Value	2.7808 mm
Use Range	No
Face/Face	Yes
Face/Edge	No
Edge/Edge	No
Priority	Include All
Group By	Bodies
Search Across	Bodies

TABLE 7
Model (A4) > Connections > Contacts > Contact Regions

Object Name	*Contact Region*	*Contact Region 2*	*Contact Region 3*	*Contact Region 4*	*Contact Region 5*	*Contact Region 6*	*Contact Region 7*	*Contact Region 8*	*Contact Region 9*	*Contact Region 10*	*Contact Region 11*
State	Fully Defined										
Scope											
Scoping Method	Geometry Selection										
Contact	3 Faces								4 Faces	1 Face	
Target	3 Faces								4 Faces	1 Face	
Contact Bodies	Solid										
Target Bodies	Solid										
Definition											
Type	Bonded										
Scope Mode	Automatic										
Behavior	Program Controlled										
Trim Contact	Program Controlled										
Trim Tolerance	2.7808 mm										
Suppressed	No										
Advanced											
Formulation	Program Controlled										
Detection Method	Program Controlled										

Penetration Tolerance	Program Controlled
Elastic Slip Tolerance	Program Controlled
Normal Stiffness	Program Controlled
Update Stiffness	Program Controlled
Pinball Region	Program Controlled
Geometric Modification	
Contact Geometry Correction	None

Mesh

TABLE 8
Model (A4) > Mesh

Object Name	*Mesh*
State	Solved
Defaults	
Physics Preference	Mechanical
Relevance	0
Sizing	
Use Advanced Size Function	Off
Relevance Center	Fine
Element Size	10.0 mm
Initial Size Seed	Active Assembly
Smoothing	Medium
Transition	Fast

Span Angle Center	Coarse
Minimum Edge Length	4.0 mm
Inflation	
Use Automatic Inflation	None
Inflation Option	Smooth Transition
Transition Ratio	0.272
Maximum Layers	5
Growth Rate	1.2
Inflation Algorithm	Pre
View Advanced Options	No
Patch Conforming Options	
Triangle Surface Mesher	Program Controlled
Patch Independent Options	
Topology Checking	Yes
Advanced	
Number of CPUs for Parallel Part Meshing	4
Shape Checking	Standard Mechanical
Element Midside Nodes	Program Controlled
Straight Sided Elements	No
Number of Retries	Default (4)
Extra Retries For Assembly	Yes
Rigid Body Behavior	Dimensionally Reduced
Mesh Morphing	Disabled
Defeaturing	
Pinch Tolerance	Please Define
Generate Pinch on Refresh	No
Automatic Mesh Based Defeaturing	On

Defeaturing Tolerance	Default
Statistics	
Nodes	175836
Elements	45446
Mesh Metric	None

Static Structural (A5)

TABLE 9
Model (A4) > Analysis

Object Name	*Static Structural (A5)*
State	Solved
Definition	
Physics Type	Structural
Analysis Type	Static Structural
Solver Target	Mechanical APDL
Options	
Environment Temperature	22. °C
Generate Input Only	No

TABLE 10
Model (A4) > Static Structural (A5) > Analysis Settings

Object Name	*Analysis Settings*
State	Fully Defined
Step Controls	
Number Of Steps	1.
Current Step Number	1.
Step End Time	1. s
Auto Time Stepping	Program Controlled
Solver Controls	

Solver Type	Program Controlled
Weak Springs	Program Controlled
Large Deflection	Off
Inertia Relief	Off
Restart Controls	
Generate Restart Points	Program Controlled
Retain Files After Full Solve	No
Nonlinear Controls	
Newton-Raphson Option	Program Controlled
Force Convergence	Program Controlled
Moment Convergence	Program Controlled
Displacement Convergence	Program Controlled
Rotation Convergence	Program Controlled
Line Search	Program Controlled
Stabilization	Off
Output Controls	
Stress	Yes
Strain	Yes
Nodal Forces	No
Contact Miscellaneous	No
General Miscellaneous	No
Store Results At	All Time Points
Analysis Data Management	

Solver Files Directory	C:\Users\user\Desktop\162656\Circular Plate\8 Bolts meshing and analysis\18mm\Concentric_files\dp0\SYS\MECH\
Future Analysis	None
Scratch Solver Files Directory	
Save MAPDL db	No
Delete Unneeded Files	Yes
Nonlinear Solution	Yes
Solver Units	Active System
Solver Unit System	nmm

TABLE 11
Model (A4) > Static Structural (A5) > Loads

Object Name	*Pressure*	*Pressure 2*	*Force*	*Fixed Support*	*Fixed Support 2*	*Fixed Support 3*	*Fixed Support 4*	*Fixed Support 5*	*Fixed Support 6*	*Fixed Support 7*	*Fixed Support 8*
State	Fully Defined										
Scope											
Scoping Method	Geometry Selection										
Geometry	1 Face		1 Vertex	1 Face							
Definition											
Type	Pressure		Force	Fixed Support							
Define By	Normal To		Components								
Magnitude	1.167e-003 MPa (ramped)	-1.167e-003 MPa (ramped)									
Suppressed	No										

Coordinate System		Global Coordinate System	
X Component		0. N (ramped)	
Y Component		0. N (ramped)	
Z Component		15000 N (ramped)	

FIGURE 1
Model (A4) > Static Structural (A5) > Pressure

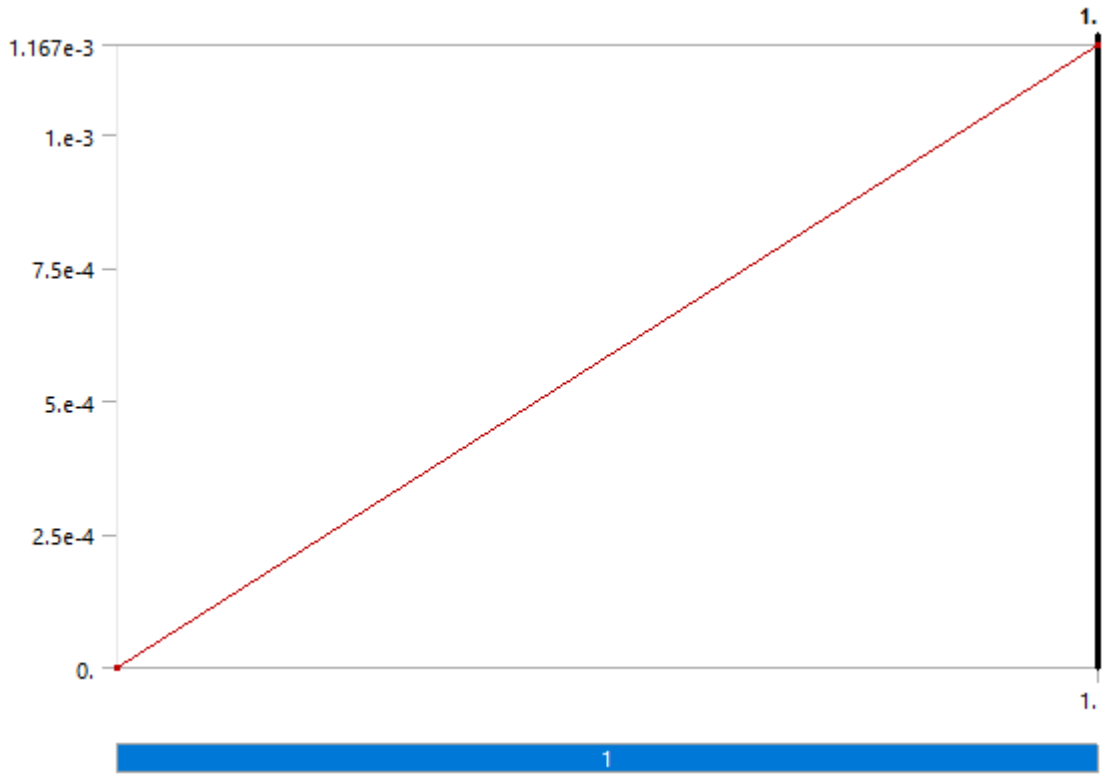

FIGURE 2
Model (A4) > Static Structural (A5) > Pressure 2

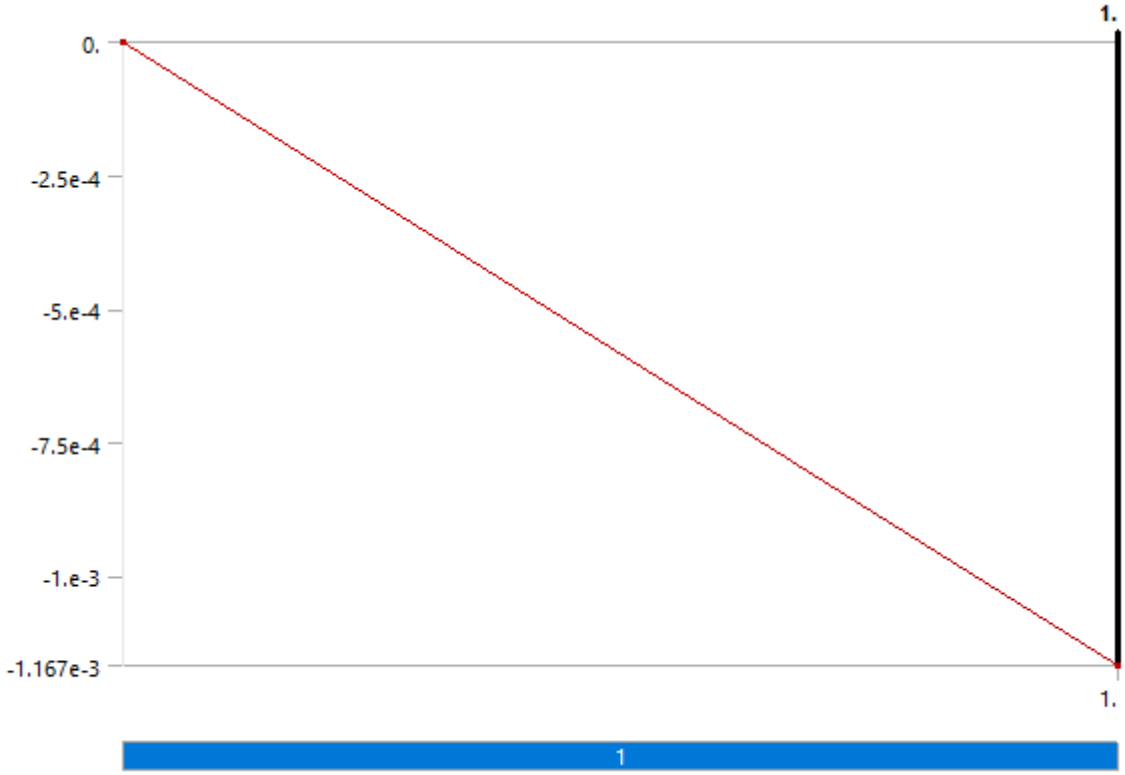

FIGURE 3
Model (A4) > Static Structural (A5) > Force

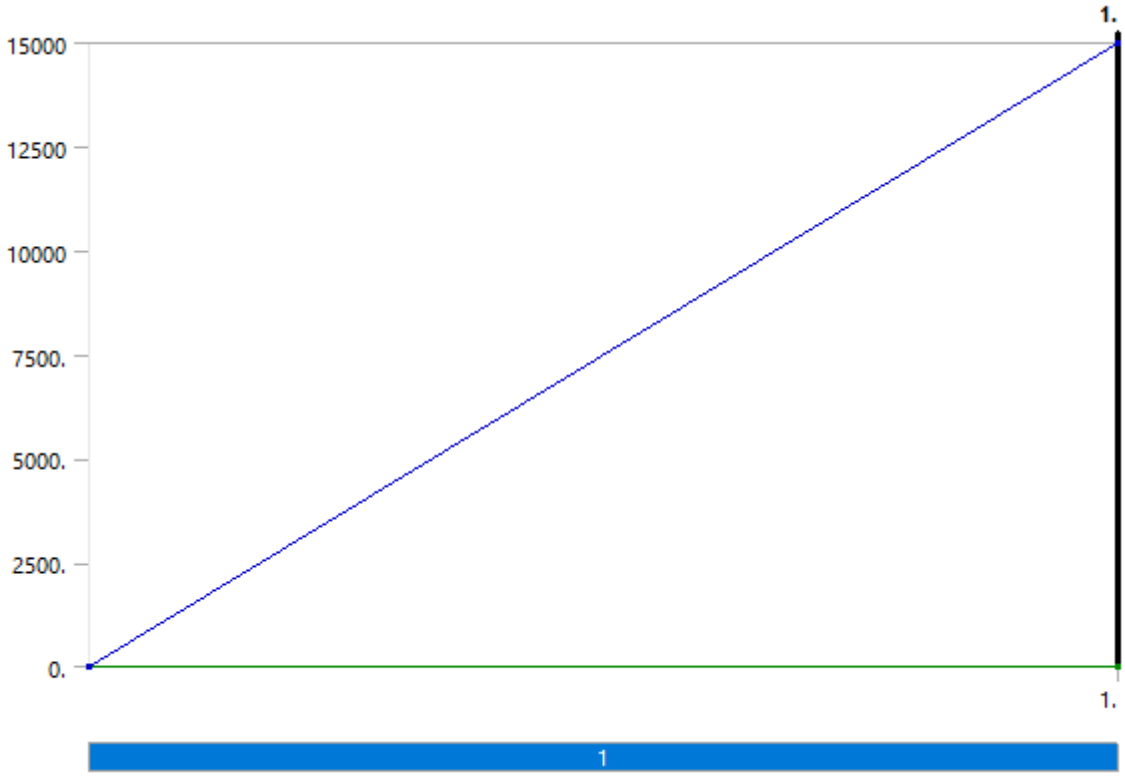

Solution (A6)

TABLE 12
Model (A4) > Static Structural (A5) > Solution

Object Name	*Solution (A6)*
State	Solved
Adaptive Mesh Refinement	
Max Refinement Loops	1.
Refinement Depth	2.
Information	
Status	Done

TABLE 13
Model (A4) > Static Structural (A5) > Solution (A6) > Solution Information

Object Name	*Solution Information*
State	Solved
Solution Information	
Solution Output	Solver Output
Newton-Raphson Residuals	0
Update Interval	2.5 s
Display Points	All
FE Connection Visibility	
Activate Visibility	Yes
Display	All FE Connectors
Draw Connections Attached To	All Nodes
Line Color	Connection Type
Visible on Results	No
Line Thickness	Single
Display Type	Lines

TABLE 14
Model (A4) > Static Structural (A5) > Solution (A6) > Results

Object Name	*Total Deformation*	*Equivalent Elastic Strain*	*Maximum Principal Elastic Strain*	*Minimum Principal Elastic Strain*	*Maximum Shear Elastic Strain*	*Equivalent Stress*	*Maximum Principal Stress*	*Minimum Principal Stress*	*Maximum Shear Stress*
State	Solved								
Scope									
Scoping Method	Geometry Selection								
Geometry	1 Body								
Definition									
Type	Total Deformation	Equivalent Elastic Strain	Maximum Principal Elastic Strain	Minimum Principal Elastic Strain	Maximum Shear Elastic Strain	Equivalent (von-Mises) Stress	Maximum Principal Stress	Minimum Principal Stress	Maximum Shear Stress
By	Time								
Display Time	Last								
Calculate Time History	Yes								
Identifier									
Suppressed	No								
Results									
Minimum	4.3147e-004 mm	6.5884e-008 mm/mm	-2.3215e-005 mm/mm	-2.1065e-004 mm/mm	8.8136e-008 mm/mm	1.2736e-002 MPa	-24.473 MPa	-43.55 MPa	6.7797e-003 MPa

Maximum	4.0242e-002 mm	2.1292e-004 mm/mm	9.8674e-005 mm/mm	1.2307e-006 mm/mm	2.8027e-004 mm/mm	41.318 MPa	25.316 MPa	2.4789 MPa	21.559 MPa
Minimum Value Over Time									
Minimum	8.6293e-005 mm	1.3205e-008 mm/mm	-2.3215e-005 mm/mm	-2.1065e-004 mm/mm	1.7667e-008 mm/mm	2.5532e-003 MPa	-24.473 MPa	-43.55 MPa	1.359e-003 MPa
Maximum	4.3147e-004 mm	6.5884e-008 mm/mm	-4.6434e-006 mm/mm	-4.2139e-005 mm/mm	8.8136e-008 mm/mm	1.2736e-002 MPa	-4.8952 MPa	-8.7122 MPa	6.7797e-003 MPa
Maximum Value Over Time									
Minimum	8.0484e-003 mm	4.2593e-005 mm/mm	1.9731e-005 mm/mm	2.4604e-007 mm/mm	5.6066e-005 mm/mm	8.2655 MPa	5.0631 MPa	0.49581 MPa	4.3127 MPa
Maximum	4.0242e-002 mm	2.1292e-004 mm/mm	9.8674e-005 mm/mm	1.2307e-006 mm/mm	2.8027e-004 mm/mm	41.318 MPa	25.316 MPa	2.4789 MPa	21.559 MPa
Information									
Time	1. s								
Load Step	1								
Substep	4								
Iteration Number	6								
Integration Point Results									
Display Option		Averaged							
Average Across Bodies		No							

FIGURE 4
Model (A4) > Static Structural (A5) > Solution (A6) > Total Deformation

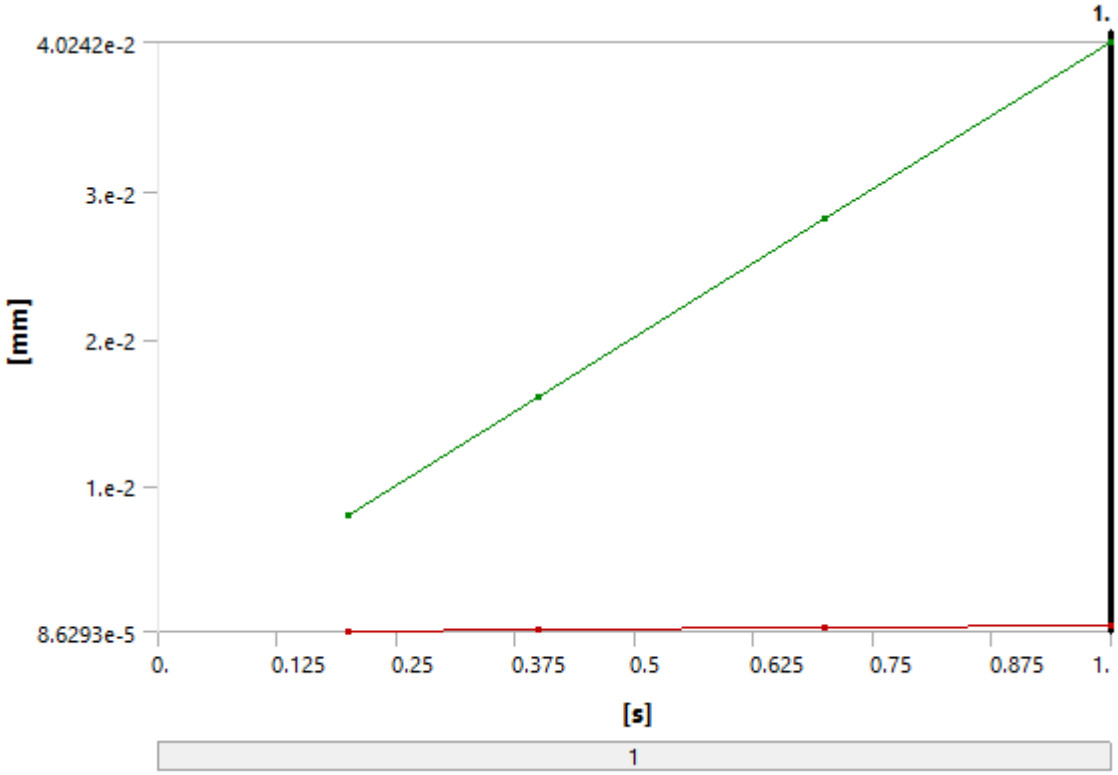

TABLE 15
Model (A4) > Static Structural (A5) > Solution (A6) > Total Deformation

Time [s]	Minimum [mm]	Maximum [mm]
0.2	8.6293e-005	8.0484e-003
0.4	1.7258e-004	1.6097e-002
0.7	3.0202e-004	2.8169e-002
1.	4.3147e-004	4.0242e-002

FIGURE 5
Model (A4) > Static Structural (A5) > Solution (A6) > Equivalent Elastic Strain

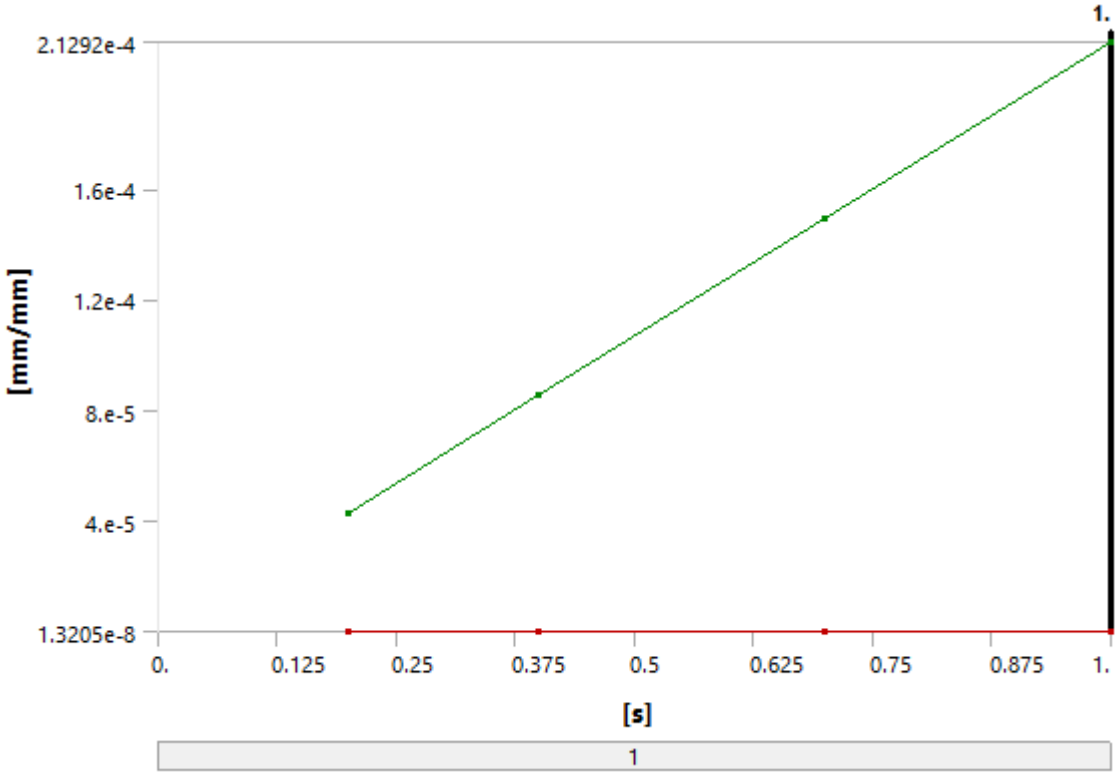

TABLE 16
Model (A4) > Static Structural (A5) > Solution (A6) > Equivalent Elastic Strain

Time [s]	Minimum [mm/mm]	Maximum [mm/mm]
0.2	1.3205e-008	4.2593e-005
0.4	2.6397e-008	8.5181e-005
0.7	4.6157e-008	1.4906e-004
1.	6.5884e-008	2.1292e-004

FIGURE 6
Model (A4) > Static Structural (A5) > Solution (A6) > Maximum Principal Elastic Strain

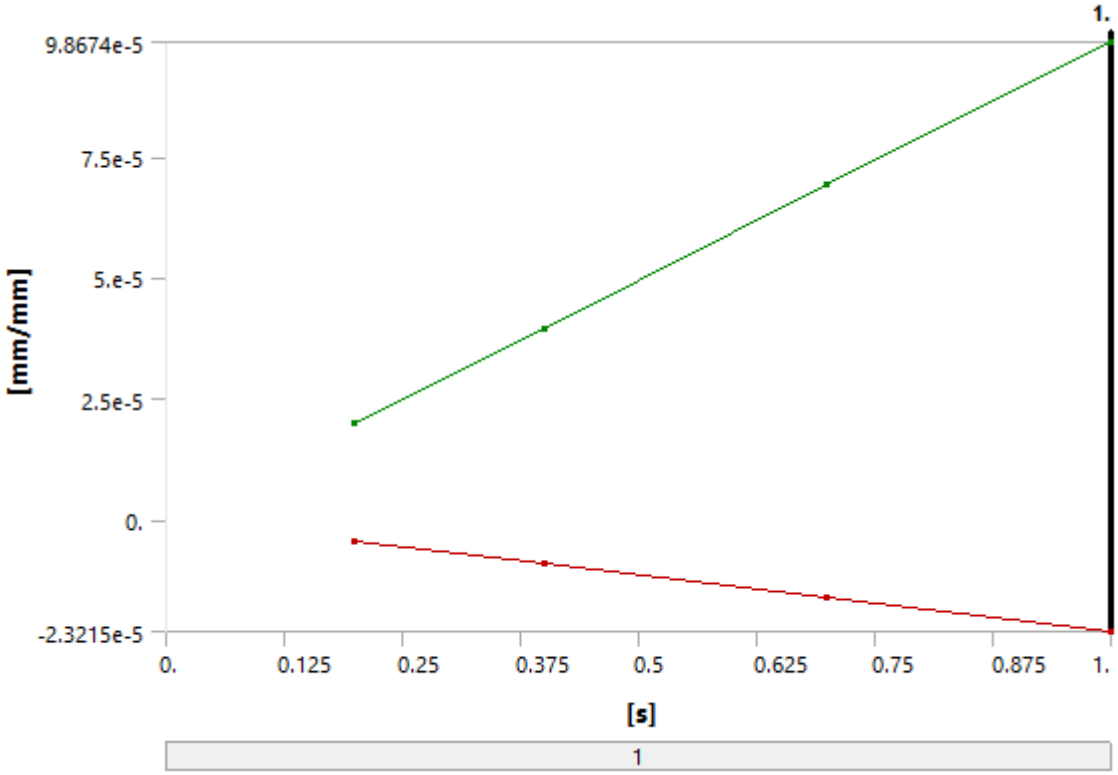

TABLE 17
Model (A4) > Static Structural (A5) > Solution (A6) > Maximum Principal Elastic Strain

Time [s]	Minimum [mm/mm]	Maximum [mm/mm]
0.2	-4.6434e-006	1.9731e-005
0.4	-9.2866e-006	3.9464e-005
0.7	-1.6251e-005	6.9067e-005
1.	-2.3215e-005	9.8674e-005

FIGURE 7
Model (A4) > Static Structural (A5) > Solution (A6) > Minimum Principal Elastic Strain

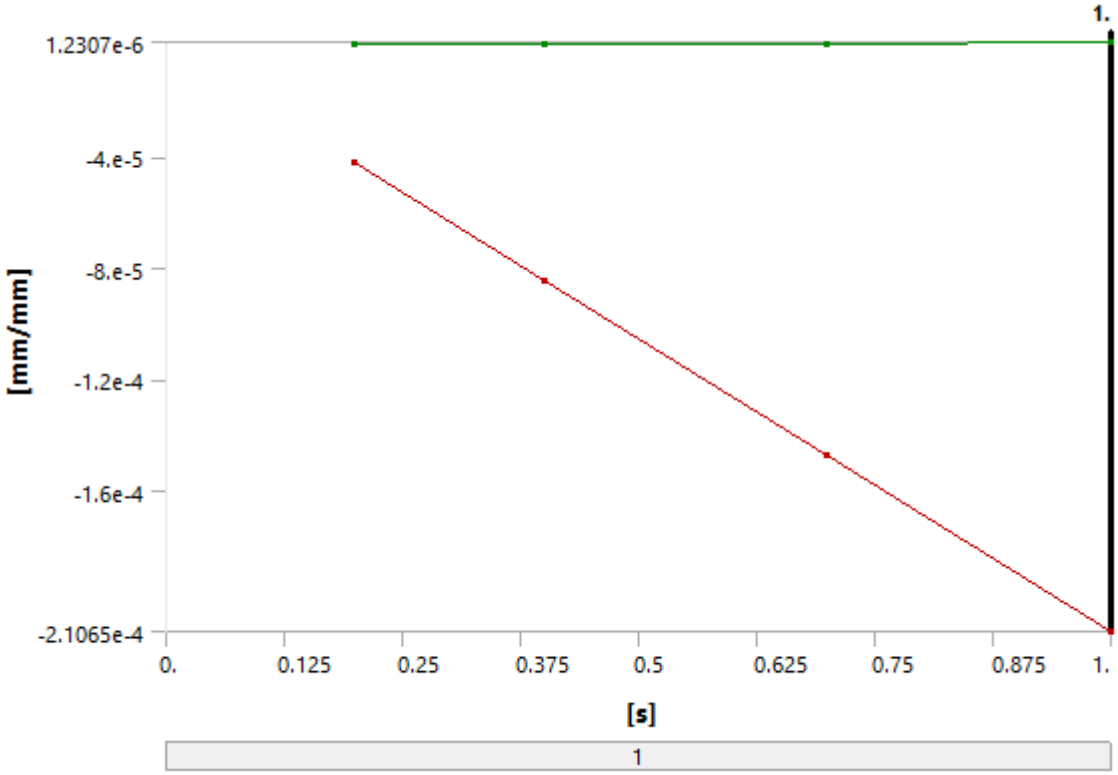

TABLE 18
Model (A4) > Static Structural (A5) > Solution (A6) > Minimum Principal Elastic Strain

Time [s]	Minimum [mm/mm]	Maximum [mm/mm]
0.2	-4.2139e-005	2.4604e-007
0.4	-8.4273e-005	4.9223e-007
0.7	-1.4747e-004	8.6145e-007
1.	-2.1065e-004	1.2307e-006

FIGURE 8
Model (A4) > Static Structural (A5) > Solution (A6) > Maximum Shear Elastic Strain

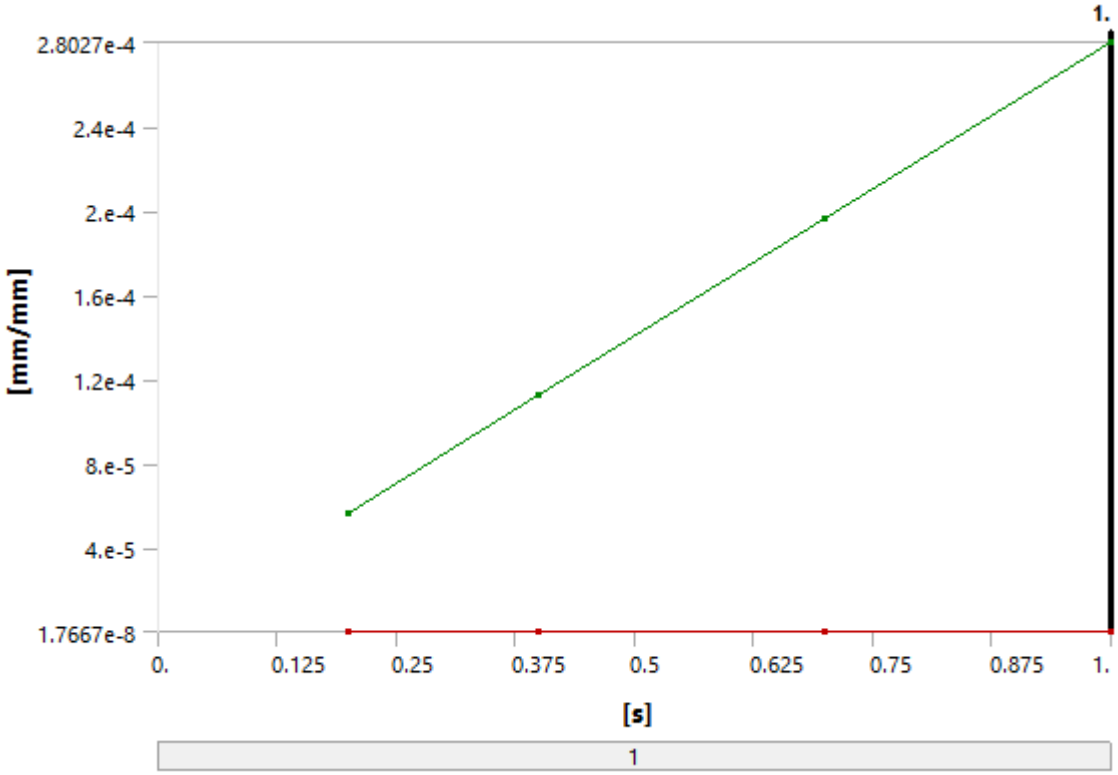

TABLE 19
Model (A4) > Static Structural (A5) > Solution (A6) > Maximum Shear Elastic Strain

Time [s]	Minimum [mm/mm]	Maximum [mm/mm]
0.2	1.7667e-008	5.6066e-005
0.4	3.5314e-008	1.1213e-004
0.7	6.1747e-008	1.962e-004
1.	8.8136e-008	2.8027e-004

FIGURE 9
Model (A4) > Static Structural (A5) > Solution (A6) > Equivalent Stress

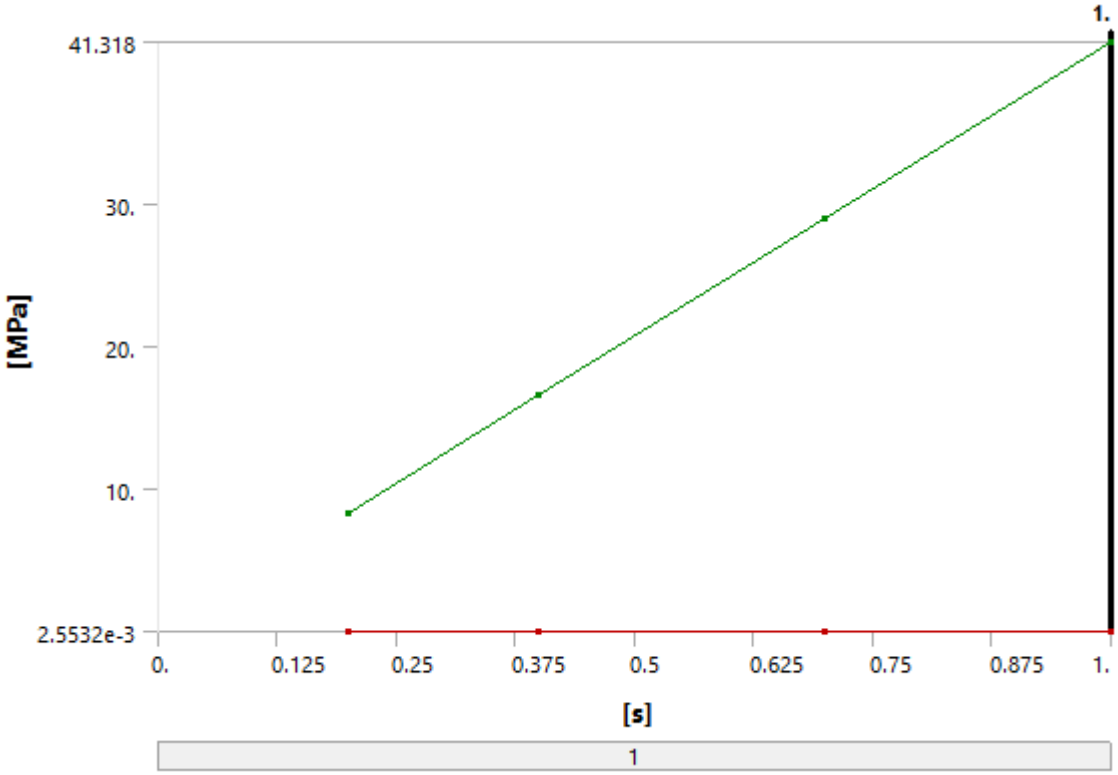

TABLE 20
Model (A4) > Static Structural (A5) > Solution (A6) > Equivalent Stress

Time [s]	Minimum [MPa]	Maximum [MPa]
0.2	2.5532e-003	8.2655
0.4	5.1034e-003	16.53
0.7	8.9229e-003	28.925
1.	1.2736e-002	41.318

FIGURE 10
Model (A4) > Static Structural (A5) > Solution (A6) > Maximum Principal Stress

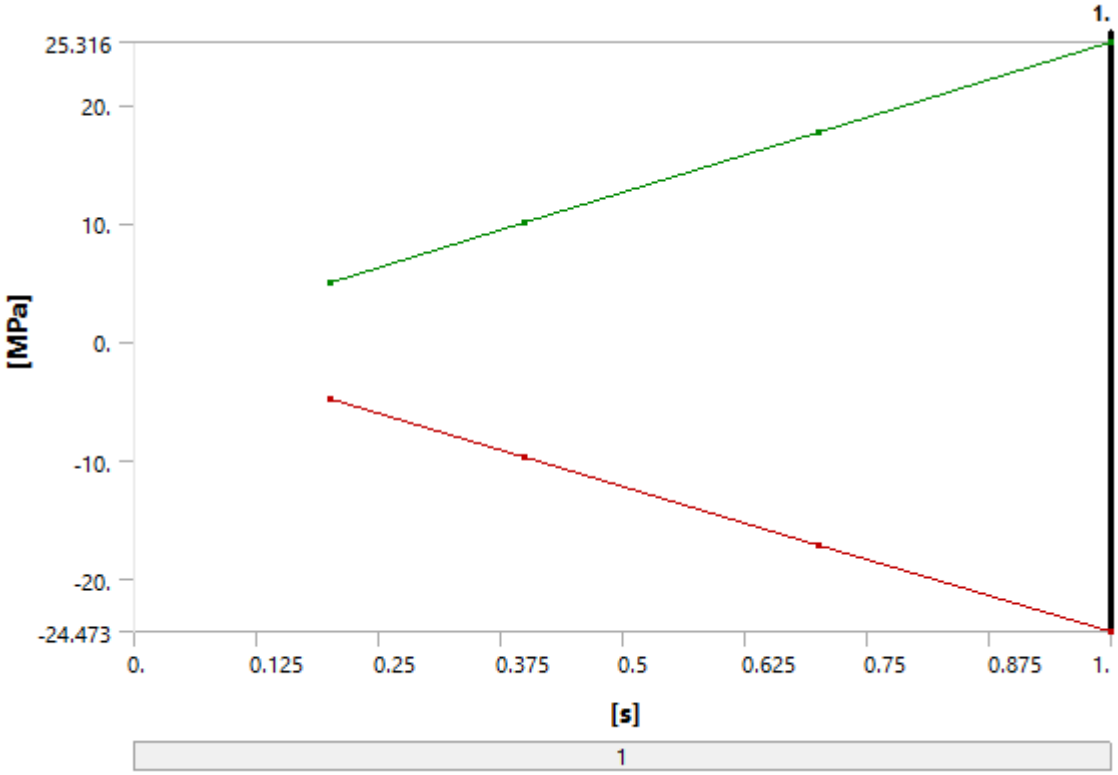

TABLE 21
Model (A4) > Static Structural (A5) > Solution (A6) > Maximum Principal Stress

Time [s]	Minimum [MPa]	Maximum [MPa]
0.2	-4.8952	5.0631
0.4	-9.7902	10.126
0.7	-17.132	17.721
1.	-24.473	25.316

FIGURE 11
Model (A4) > Static Structural (A5) > Solution (A6) > Minimum Principal Stress

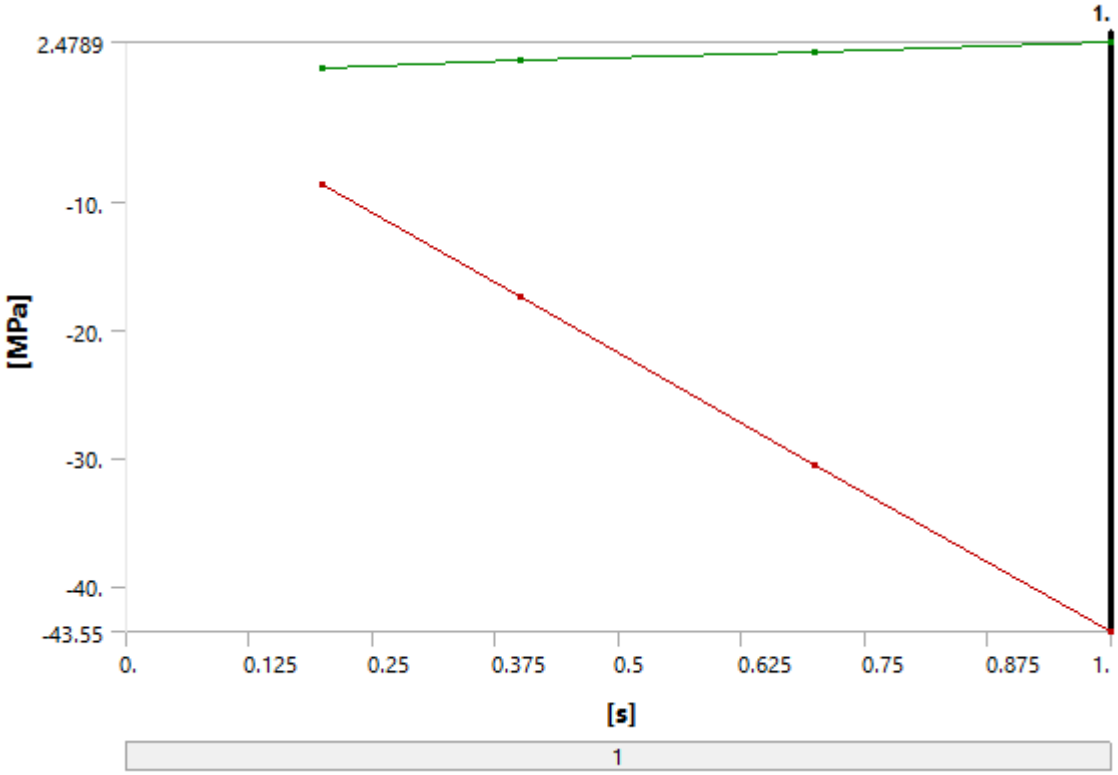

TABLE 22
Model (A4) > Static Structural (A5) > Solution (A6) > Minimum Principal Stress

Time [s]	Minimum [MPa]	Maximum [MPa]
0.2	-8.7122	0.49581
0.4	-17.423	0.9916
0.7	-30.488	1.7353
1.	-43.55	2.4789

FIGURE 12
Model (A4) > Static Structural (A5) > Solution (A6) > Maximum Shear Stress

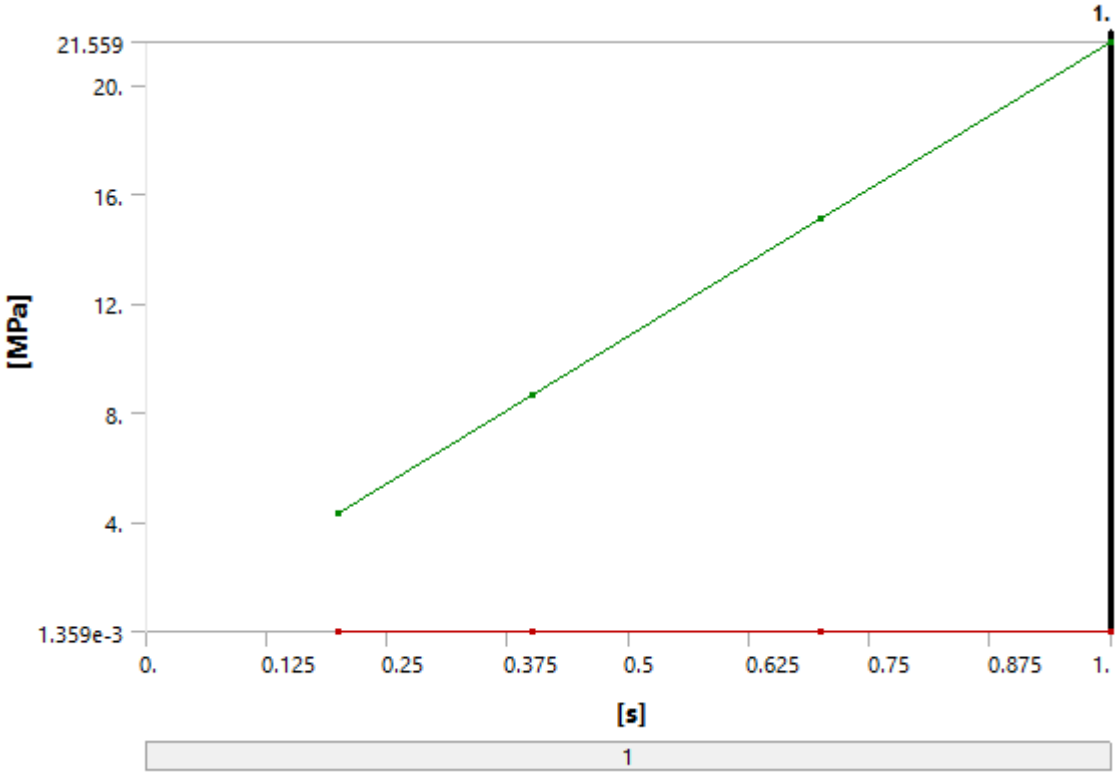

TABLE 23
Model (A4) > Static Structural (A5) > Solution (A6) > Maximum Shear Stress

Time [s]	Minimum [MPa]	Maximum [MPa]
0.2	1.359e-003	4.3127
0.4	2.7165e-003	8.625
0.7	4.7498e-003	15.093
1.	6.7797e-003	21.559

Material Data

Structural Steel NL

TABLE 24
Structural Steel NL > Constants

Density	7.85e-009 tonne mm^-3
Specific Heat	4.34e+008 mJ tonne^-1 C^-1

TABLE 25
Structural Steel NL > Isotropic Elasticity

Temperature C	Young's Modulus MPa	Poisson's Ratio	Bulk Modulus MPa	Shear Modulus MPa
	2.e+005	0.3	1.6667e+005	76923

TABLE 26
Structural Steel NL > Bilinear Isotropic Hardening

Yield Strength MPa	Tangent Modulus MPa	Temperature C
250	1450	

Concrete NL

TABLE 27
Concrete NL > Constants

Density	2.3e-009 tonne mm^-3

TABLE 28
Concrete NL > Drucker-Prager Strength Piecewise

Pressure P MPa	Yield Stress Y MPa
-4	0
0	10
15	40
50	44

TABLE 29
Concrete NL > Tensile Pressure Failure

Maximum Tensile Pressure MPa
-4

TABLE 30
Concrete NL > Crack Softening Failure

Fracture Energy Gf mJ mm^-2
0.1

TABLE 31
Concrete NL > Isotropic Elasticity

Temperature C	Young's Modulus MPa	Poisson's Ratio	Bulk Modulus MPa	Shear Modulus MPa
	30000	0.18	15625	12712

FIGURE 13
Model (A4) > Static Structural (A5) > Solution (A6) > Minimum Principal Stress

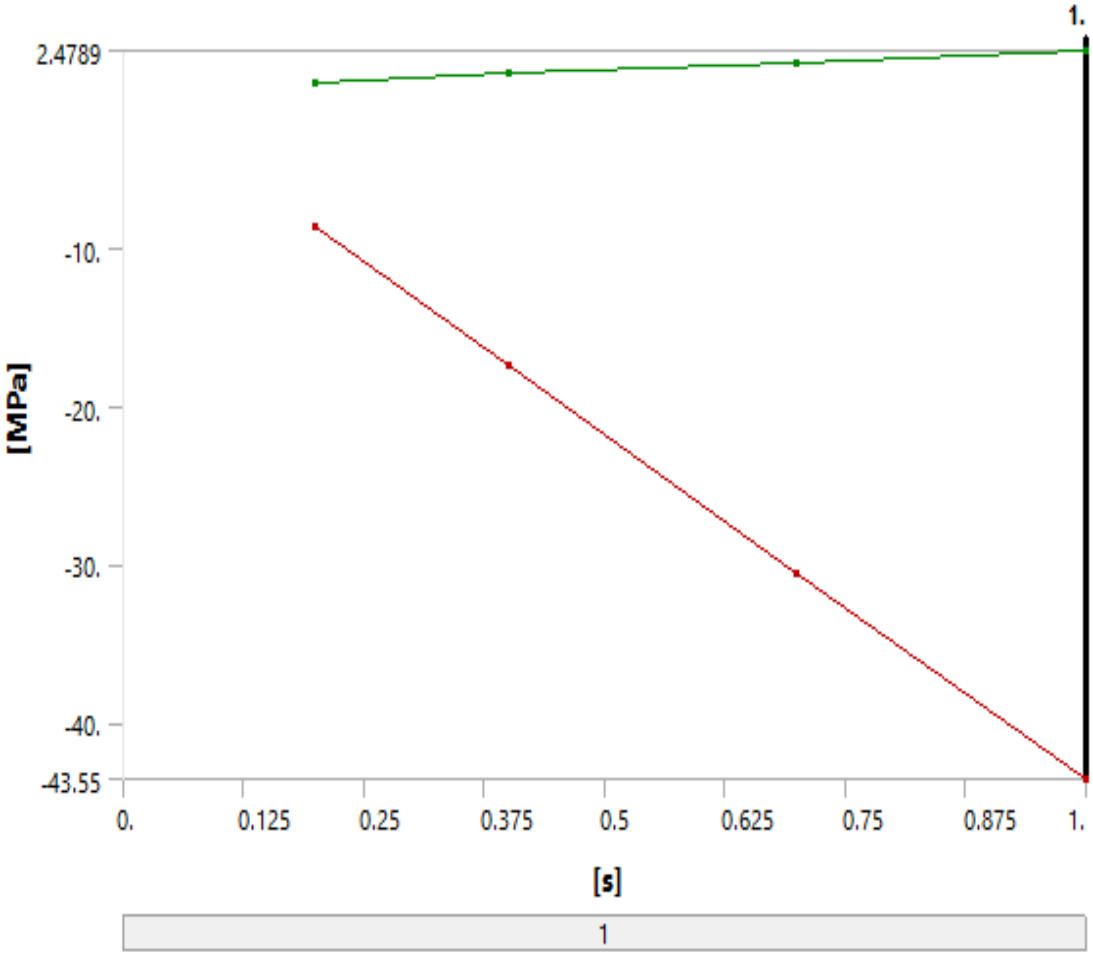

FIGURE 14
Model (A4) > Static Structural (A5) > Solution (A6) > Maximum Shear Stress

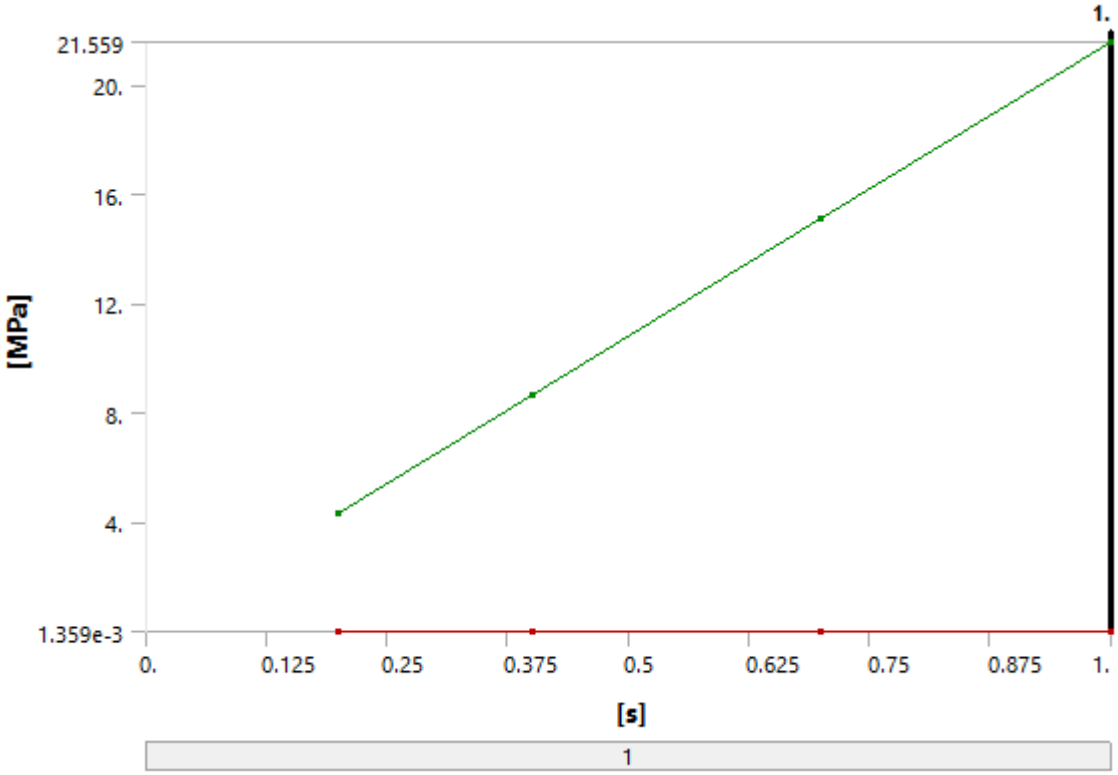

JAYPEE UNIVERSITY OF INFORMATION TECHNOLOGY, WAKNAGHAT
LEARNING RESOURCE CENTER

PLAGIARISM VERIFICATION REPORT

Date: 10.05.2018

Type of Document (Tick): Thesis | M.Tech Dissertation/ Report ✓ | B.Tech Project Report | Paper

Name: SUMER R SINGH Department: CIVIL ENGINEERING

Enrolment No. 162656 Registration No. 162656

Phone No. 9805107933 Email ID. SumerSinghOOR@hotmail.com

Name of the Supervisor: Mr. Kaushal Kumar.

Title of the Thesis/Dissertation/Project Report/Paper (In Capital letters): COMPARITIVE NONLINEAR FINITE ELEMENT ANALYSIS OF SQUARE AND CIRCULAR STEEL BASE PLATE ON LEVELING NUTS USING ANSYS.

Kindly allow me to avail Turnitin software report for the document mentioned above.

(Signature)

FOR ACCOUNTS DEPARTMENT:

Amount deposited: Rs. 500/- Dated: 10.5.18 Receipt No. BAN1805Y264

(Enclosed payment slip)

(Account Officer)

FOR LRC USE:

The above document was scanned for plagiarism check. The outcome of the same is reported below:

Copy Received on	Report delivered on	Similarity Index in %	Submission Details	
10/05/2018	11/05/2018	18%	Word Counts	14,012
			Character Counts	71,120
			Page counts	82
			File Size	1.97M

Checked by
Name & Signature

Librarian

LIBRARIAN
LEARNING RESOURCE CENTER
Jaypee University of Information Technology
Waknaghat, Distt, Solan (Himachal Pradesh)
Pin Code: 173234

turnitin

Digital Receipt

This receipt acknowledges that Turnitin received your paper. Below you will find the receipt information regarding your submission.

The first page of your submissions is displayed below.

Submission author:	Sumer R Singh
Assignment title:	MTech Project Reports
Submission title:	"COMPARITIVE NONLINEAR FINITE..
File name:	M.Tech_Sumer_162656.pdf
File size:	1.97M
Page count:	82
Word count:	14,012
Character count:	71,120
Submission date:	11-May-2018 10:48AM (UTC+0530)
Submission ID:	962266156

"COMPARITIVE NONLINEAR FINITE ELEMENT ANALYSISOF SQUARE AND CIRCULAR STEEL BASE PLATE ON LEVELING NUTS USING ANSYS"

A Thesis

Submitted in partial fulfillment of the requirements for the award of the degree of

MASTER OF TECHNOLOGY

IN

CIVIL ENGINEERING

With specialization in

STRUCTURAL ENGINEERING

Under the supervision of

Dr. Ashok Kumar Gupta

(Head of Department)

&

Mr. Kaushal Kumar

(Assistant Professor)

By

Sumer R Singh

(162656)

To

JAYPEE UNIVERSITY OF INFORMATION TECHNOLOGY

WAKNAGHAT, SOLAN – 173 234

HIMACHAL PRADESH, INDIA

MAY-2018

LIBRARIAN
LEARNING RESOURCE CENTER
Jaypee University of Information Technology
Waknaghat, Distt. Solan (Himachal Pradesh)
Pin Code. 17323[illegible]